We thank the reviewers for their reviews and recommendation to publish. We have considered every point and corrected the paper to include their points. The referees comments are in black, responds from the authors are in blue and revised text are in red.

Report #1
[Specific comments]

1. The authors now explicitly argue that "the solid-state solution of nitrate molecules can occur concurrently with surface adsorption" (L150-151). If I understand correctly, the present model formulation dictates that a thermodynamic limitation does not exist anymore once HNO3 is retained on/in the outermost layer of their hypothesized spherical ice grain. As such, HNO3 trapped on the ice surface via Langmuir adsorption is assumed to be transferred instantaneously across the depth of the order of several micrometers to the outermost layer of bulk ice and subject to solid-state diffusion further inside based on the diffusivity having been determined experimentally. I am inclined to disagree to the claim that this model formulation is entirely based upon the first principles.

To avoid confusion we now emphasize throughout the paper that the models are based on physical paramaterisations and laboratory data.

A clarification has been added to the text (See below in red) in Section 3.1.3 (line 312-317) to explain what boundary conditions are used.

"The concentration gradient between the grain boundary and its centre drives solid state diffusion of nitrate within the bulk ice. The NO_3^- concentration profile within the snow grain can be found by solving the following partial differential equation

$$\frac{\partial U(r)}{\partial t} = k_{diff}\left(\frac{\partial^2 U(r)}{\partial r^2}\right)$$

where U(r) is the concentration at distance r from the centre of the snow grain and k_{diff} is the solid-state diffusion coefficient, which is assumed to be homogeneous across the snow grain. The nitrate concentration at the centre is set to U(0) = 0 and at the grain boundary $U(R_{eff}) = [HNO_3(surf)]$ is defined by surface adsorption and co-condensation at temperatures below To (Eq. 7) or by solvation into the infinitesimal DI at temperature above To (Eq. 13)."

2. It appears to me that the treatment of the surface to bulk mass transfer of HNO3 is even more problematic in "Model 1" where the authors assume that HNO3 dissolved in the DI is subject to solid-state diffusion into the bulk volume of ice without thermodynamic limitation. This assumption effectively asserts that the equilibrium solubility of HNO3 in the entire volume of solid ice is identical to that in the liquid-like DI. Does any of the earlier studies advocating the role of DI assume such an equivalence between the DI and the bulk ice? So I still feel that the present study does not really offer the refutation of the HNO3 uptake onto the DI as a viable process.

The text has been clarified in Sect 3.1 (line 216-230) about the assumptions made regarding the DI in this paper.

'The physical properties of the DI, such as the layer thickness, partitioning coefficient, diffusivity etc., are still poorly understood. The laboratory

measurements of thickness of DI of pure ice range from a monolayer of water to around a few hundreds of nm (Bartels-Rausch et al., 2014) depending on the measuring techniques and temperature. Thur there is no parameterisation available to estimate the thickness of DI as a function of temperature and/or concentration within the bulk. Also, no measured 230 values are available for the air-DI partitioning and the diffusivity of the DI. Therefore, for the DI in Model 1 has the following is assumed: 1) the partitioning between air and the DI is governed by Henry's law; 2) the DI is interacting with the bulk ice, which the nitrate molecules solvated into the DI are allowed to diffused into the bulk ice, the rate of the transport is limited by the diffusivity of solid ice; 3) the DI has an infinitesimal thickness and the concentration in the DI is acting as the boundary condition of the solid-state diffusion into the snow grain (See Sect. 3.1.3).
Note that besides adopting Henry's law coefficient as the partitioning coefficient of the DI, the other assumptions made here for the DI is different from the assumptions made by previous models (e.g. Thomas et al., 2011; Toyota et al., 2014) that often assume the DI has a certain arbitrary thickness.'

3. In section 5.1.1, the authors refer to their model results based upon "Kinetic approach" and "Equilibrium approach" suggested earlier by Bock et al. (2016). These models are not exactly the same as the standard suite of models, "Model 1" and "Model 2", in the present study. Hence the authors are apparently nudged to the names of the models used in Bock et al. (2016). I was confused when I first read this paper and again when I read the revised manuscript, partly because the transfer of HNO3 into liquid micro-pockets is treated by equilibrium in "Model 2". I would rather like the authors to streamline the naming convention so that the "Kinetic" and "Equilibrium" models referred to here are called by numbers. For example, the "Kinetic" model can be a sub-category of "Model 1". It is of course still useful to refer to the fact that these models are based on the "Kinetic" and "Equilibrium" approaches by Bock et al. (2016). Also, I would have liked it if the authors had introduced and discussed Eq. (19) in section 3, even though it does not belong to their standard model formulation.
Theses are good suggestions: the equation Eq. (19) after Bock et al. 2016 approach is now moved to Sect. 3 and their approach is referred as the 'Bock-BC1' and the kinetic approach taken in this study is now referred as the 'Model 1-BCice', where BC stand for "boundary condition".

[Minor comments and technical suggestions]

L70-71, "Murray et al., 2015; 3)": An apparent typo.
Yes, this has been corrected
L77-78: Please double check if this sentence makes sense.
Yes, this has been corrected, now written as "The bulk concentration of H_2O_2 is determined by solid-state diffusion of H_2O_2 while the bulk concentration of HCHO is determined by linear isotherm adsorption of HCHO on ice."

L86: dynamicS
Yes, this has been corrected

L177: “a 2” -> “two”
Yes, this has been corrected

L178: “one” -> “an”
Yes, this has been corrected

L241: “… growth law described by Flanner and Zander (2006):”
Yes, this has been corrected

L334: below THE freezing POINT
Yes, this has been corrected

L354: “particulate nitrate” -> “total particulate and gaseous nitrate” (?)
Yes, this has been corrected as “atmospheric nitrate”

L389: well-mixed SO that
Yes, this has been corrected

L425: Cv(RMSE) = 0.73 (Table 4)
Yes, this has been corrected

L508: “inf” -> “in”
Yes, this has been corrected

L512-513: “surface, layer leading to” -> “surface layer, leading to”
Yes, this has been corrected

L513: “find in a more stable” -> “found in the particulate”
Yes, this has been corrected

L522: information IS AVAILABLE on
Yes, this has been corrected

L525 & L550: “maybe” -> “may be”
Yes, this has been corrected

L581: requireD
Yes, this has been corrected

L599 & L670: “larger” -> “higher”
Yes, this has been corrected

L665: “sensitivity” -> “sensitive”
Yes, this has been corrected

Table 1: Mathematical expressions (second column) for “Interfacial mass transport to a liquid phase” and “Gas-phase diffusion to the surface of a spherical droplet” should be inverted.

Yes, this has been corrected

Report #2

The authors have performed an interesting modeling study of an important and valuable dataset. The technical work is a worthwhile contribution to the literature; some new approaches are introduced and reasonable agreement with field data is achieved. However, the results are not currently presented in a manner that is acceptable for publication. The authors disparage previous work in the text for requiring tuning parameters and unrealistic assumptions. This is a fair criticism of nearly all modeling studies in this field, since fundamental understanding lags significantly behind our needs for process modeling, and therefore assumptions are required.

The problem is that the authors present their modeling approaches as being superior to previous work without acknowledging up front the great uncertainty surrounding several of the "first principals" assumptions made in this study.
To avoid confusion, we now emphasize the models developed here are based on physical paramaterisations and laboratory data. This paper has been edited throughout to reflect this.

It is not my intention to call out these assumptions as erroneous, but rather to insist that the authors acknowledge them and discuss the uncertainties that they introduce. For example, in model 1: The range of the DI onset temperature, To, is based on experimental data, but it should be acknowledged that this is a type of tuning parameter.

We agree in considering the uncertainties is important, thus, the uncertainties presented in reported for experimental observations are considered in a sensitivity analysis in Sect 6.5.

However, threshold temperature T_0 is a parameter with physical meaning. Therefore, it is not an arbitrary tuning parameter. It is varied within the range of available experimental data, which might be narrowed in the future. The model uncertainties due to the uncertainty in the T_0 is explored in a sensitivity test presented in Sect 6.5.

Another assumption must be made regarding the depth/volume of the DI, although I did not see this discussed in the text. Uptake of HNO3 to the DI is assumed (as it is in nearly all snowpack modeling studies, for lack of a better option) to follow Henry's Law for bulk aqueous solutions, where in reality there is no physical basis for this assumption.
The DI in this study is assumed to have an infinitesimal thickness. Other assumptions made regard to the DI in this study have now been clarified in Sect. 3.1 (line 216-230)
'The physical properties of the DI, such as the layer thickness, partitioning coefficient, diffusivity etc., are still poorly understood. The laboratory measurements of thickness of DI of pure ice range from a monolayer of water to around a few hundreds of nm (Bartels-Rausch et al., 2014) depending on the measuring techniques and temperature. Thur there is no parameterisation available to estimate the thickness of DI as a function of temperature and/or

concentration within the bulk. Also, no measured 230 values are available for the air-DI partitioning and the diffusivity of the DI. Therefore, for the DI in Model 1 has the following is assumed: 1) the partitioning between air and the DI is governed by Henry's law; 2) the DI is interacting with the bulk ice, which the nitrate molecules solvated into the DI are allowed to diffused into the bulk ice, the rate of the transport is limited by the diffusivity of solid ice; 3) the DI has an infinitesimal thickness and the concentration in the DI is acting as the boundary condition of the solid-state diffusion into the snow grain (See Sect. 3.1.3).
Note that besides adopting Henry's law coefficient as the partitioning coefficient of the DI, the other assumptions made here for the DI is different from the assumptions made by previous models (e.g. Thomas et al., 2011; Toyota et al., 2014) that often assume the DI has a certain arbitrary thickness.'

For model 2, eq. 4, which was developed assuming that the liquid solution is ideal and does not take into account partitioning of nitrate between the gas, liquid, and solid phases, is applied without discussion.
In Model 2, the partitioning of nitrate between air and ice is included as shown in the first term of Eq. 17, which reference back to Sect 3.1.1 as the same air-ice processes were applied.
In Section 3.2, the following lines been edited (line 341-457)
"The term '$\Sigma[NO_3^-](r)\ V(r) / V_{grain}$' in Eq. 17 is representing the nitrate concentration in the ice-phase and is applied to all temperatures below the melting temperature, T_m. At $T<T_m$, HNO3 can be adsorbed/desorbed and co-condensed/co-sublimated from the ice surface as was the case in Model 1 when $T <T_o$ (Sect. 3.1.1). The adsorbed and co-condensed molecules on the ice surface then diffuse into or out of the bulk ice depending on the concentration gradient of nitrate anion as was the case in Model 1 (Sect. 3.1.3). The nitrate in the snow grain contributed by these processes is referred to as the ice-phase nitrate."
and line 351-353
"The liquid in the micropocket is assumed to be ideal and the partitioning between air and liquid micropocket is described by Henry's Law (Eq. 5). This implies instantaneous equilibrium between air and liquid pocket, and is justified because;…"

In Section 6.4, the following line (722-734) been added
'Moreover, the liquid in the micropocket is assumed to behave ideally and, therefore, Henry's coefficient is used to describe the partitioning between air and the micropocket. In reality, there may be some deviation from ideality as the concentration of solutes in the micropocket is likely to be too large to be considered as an ideal dilute solution. The non-ideality should be accounted for in terms of activity coefficient, γ . At equilibrium, the relationship between a solute B and the solvent can be expressed as follow (Sander, 1999):

$$K_B = \frac{\gamma_B x_B}{P_B}$$

where P_B is the vapour pressure of B, γ_B is the activity coefficient of B and x_B is the mole fraction of B. The value of the activity coefficient approaches unity as the mole fraction of B approaches zero ($\gamma_B \rightarrow 1$ as $x_B \rightarrow 0$) and, under such ideal-dilute condition, the equilibrium constant, K_B , is defined as Henry's

coefficient. Values of activity coefficient can be found experimentally. The available parameterisation of activity coefficient of HNO_3(aq), H^+ and NO_3^- is only accurate for concentration up to 28 m (Jacobson , 2005). When the molarity is higher than ~4-5 m, depending on the temperature, the activity coefficient of H+ and NO_3^- increases as molarity increase. The concentration of the micropocket is estimated based on the parameterisation by Cho et al. (2002), which predicts a concentration a lot larger than the limit of activity coefficient parameterisation available at present. Hence, it is not possible to quantify the uncertainties caused by assuming the micropocket has ideal-solution behaviour. If the relationship between activity coefficient and molarity extend to larger molarity than 28 m, the activity coefficient would be larger than 1 and hence reduces the value of the equilibrium constant, K_B, compared to the Henry's Law coefficient. By means, the assumption of ideal-solution behaviour of micropocket is likely to overestimate the concentration of the micropocket. The activity coefficient of highly concentrated solution is needed to be found by further experimental studies. '

The authors should also take care to acknowledge when aspects of their models are adopted from or are similar to previous modeling studies, in addition to highlighting their innovations.

Previous modeling studies had been acknowledge, for example
1. Abstract, line 16 – 18: "It is therefore suggested that in winter air-snow interactions of nitrate are determined by non-equilibrium surface adsorption and co-condensation on ice coupled with solid-state diffusion inside the grain, similar to Bock et al. (2016)."
2. Introduction, line 103-104: "NO_3^- concentration is defined by non-equilibrium solvation into the DI based on Henry's coefficient, which is similar to the approach taken by other models (e.g. Thomas et al., 2011; Toyota et al., 2014)."
3. Sect. 3.1, line 206-208: "In Model 1, the uptake of HNO3 is treated as a two-step process consisting of interfacial mass trans- port across the air-snow grain boundary and subsequent diffusion into the bulk, similar approach taken by Bock et al. (2016)."

Manuscript prepared for Atmos. Chem. Phys.
with version 2014/09/16 7.15 Copernicus papers of the LaTeX class copernicus.cls.
Date: 27 July 2017

Modeling the Physical Multi-Phase Interactions of HNO_3 Between Snow and Air on the Antarctic Plateau (Dome C) and coast (Halley)

Hoi Ga Chan[1,2], Markus M. Frey[1], and Martin D. King[2]

[1]British Antarctic Survey, Natural Environment Research Council, Cambridge, CB3 0ET,UK
[2]Department of Earth Sciences, Royal Holloway University of London, Egham, Surrey, TW20 0EX, UK

Correspondence to: Hoi Ga Chan
(hohan47@bas.ac.uk)

Abstract. Emission of nitrogen oxide (NO_x = NO + NO_2) from the photolysis of nitrate (NO_3^-) in snow affect the oxidising capacity of the lower troposphere especially in remote regions, of high latitudes with little pollution. Current air-snow exchange models are limited by poor understanding of processes and often require unphysical tuning parameters. Here, two ~~physical~~ multi-phase models were developed from ~~first principles~~ physically-based parameterisations to describe the interaction of nitrate between the surface layer of the snowpack and the overlying atmosphere. The first model is similar to previous approaches and assumes that below a threshold temperature, T_o, the air-snow grain interface is pure ice and above T_o, a disordered interface (DI) emerges covering the entire grain surface. The second model assumes that air-ice interactions dominate over all temperatures below melting of ice and that any liquid ~~is concentrated in micropockets~~ present above the eutectic temperature is concentrated in micropockets. The models are used to predict the nitrate in surface snow ~~with available~~ constrained by year-round observations of mixing ratios of nitric acid in air at a cold site on the Antarctic Plateau (Dome C, $75°06'S, 123°33'E$, 3233 m a.s.l.) and at a relatively warm site on the Antarctic coast (Halley, $75°35'S, 26°39'E$, 35 m a.s.l). The first model agrees reasonably well with observations at Dome C ($C_v(RMSE)$ = 1.34), but performs poorly at Halley ($C_v(RMSE)$ = 89.28) while the second model reproduces with good agreement observations at both sites ($C_v(RMSE)$ = 0.84 at both sites). It is therefore suggested that in winter air-snow interactions of nitrate are determined by non-equilibrium surface adsorption and co-condensation on ice coupled with solid-state diffusion inside the grain, similar to Bock et al. (2016). In summer, however, the air-snow exchange of nitrate is mainly driven by solvation into liquid micropockets following Henry's law with contributions to total surface snow NO_3^- concentrations of 75% and 80% at Dome C and

Halley respectively. It is also found that the liquid volume of the snow grain and air-micropocket partitioning of HNO_3 are sensitive to both the total solute concentration of mineral ions within the snow and pH of the snow. The second model ~~can be used~~ provides an alternative method to predict nitrate concentration in the surface snow layer which is applicable over the entire range of environmental conditions typical for Antarctica and forms a basis for a future full 1D snowpack model as well as parameterisations in regional or global atmospheric chemistry models.

1 Introduction

Emissions of nitrogen oxides, NO_x = NO + NO_2, from snow to the overlying air as a result of photolysis of the nitrate anion, NO_3^-, within snow have been observed in polar (Jones et al., 2001; Beine et al., 2002) and midlatitude regions (Honrath et al., 2000). They were found to have a significant impact on the oxidising capacity of the atmospheric boundary layer, especially in remote areas, such as the polar regions, where anthropogenic pollution is small (Grannas et al., 2007). The cycling of NO and NO_2 in the troposphere alters the concentration of tropospheric ozone, O_3, partitioning of hydroxy radicals, HO_x, and organic peroxy radicals, RO_x. Tropospheric ozone is a pollutant and a greenhouse gas, and changes in the concentration can impact the regional energy balance and therefore climate (Fowler et al., 2008). Conversely, HO_x radicals are responsible for removal of many atmospheric pollutants (e.g. Gligorovski et al., 2015), such as the greenhouse gas methane, and RO_x radicals play an important role in the oxidation of volatile organic compounds (VOCs). ~~Moreover, the~~ Furthermore, NO_x emission from NO_3^- in snow imply post-depositional ~~nitrate loss from snowpacks in complicated~~ loss of NO_3^-, which complicates the interpretation of ~~polar ice core nitrate. To extract paleoclimatic information from the ice core, the interactions between the atmosphere and the snowpack need to be understood.~~ NO_3^- measured in polar ice cores (Wolff et al., 2008; France et al., 2011).

The exchange of nitric acid, HNO_3, between the atmosphere or snow interstitial air (SIA) and snow grains is complex, and is controlled by chemical and physical processes. The relative contribution of ~~the chemical~~ photochemical and physical processes has been a matter of debate (Röthlisberger et al., 2000). Isotopic studies ~~(Frey et al., 2009; Erbland et al., 2013) have shown~~ have shown that photolysis of NO_3^- is the dominating loss process of NO_3^- in snow (Frey et al., 2009; Erbland et al., 2013). Based on a typical photolysis rate coefficient of nitrate, $J_{NO_3^-} \approx 1 \times 10^{-7}\ s^{-1}$ (at the surface in Dome C at a solar zenith angle of 52°, ~~France et al. (2011)~~France et al., 2011), the characteristic time for nitrate photolysis is $\sim 10^7$ s. ~~The~~ Thus, the characteristic time of nitrate photolysis is much larger compared to other physical processes near the snowpack surface, such as grain surface adsorption and solid-state diffusion (Table 1). ~~The~~ At the top few mm of snowpack, hereafter called the skin layer and the focus region of snowpack in this paper, the physical uptake of nitrate is much quicker than the ~~chemical~~ photochemical loss due to the availability of nitric acid at the snowpack surface.

Therefore, it is assumed that the ~~chemical~~ photochemical processes are negligible and consider only the physical processes. The skin layer is defined as the top 4 mm of the snowpack, which is the depth of which the surface snow nitrate samples were collected at Dome C (Sect. 4.1).

The ~~physical exchange of nitric acid, , between the atmosphere or snow interstitial air (SIA) and snow grain are complex~~ snow grain and the air around it form together a complex multiphase interface (Bartels-Rausch et al., 2014). Gaseous HNO_3 can be taken up by different reservoirs in snow, for example the molecule can 1) adsorb on the ice surface; 2) diffuse into the ice crystal and form solid solution; 3) co-condense to the growing ice or 4) dissolve into the liquid solution located in grain boundaries, grooves at triple junctions or quadruple points. ~~Therefore, the air and snow grain form a complex multiphase interface (Bartels-Rausch et al., 2014).~~

Air-snow models have been developed to predict the exchange of trace gases between the snowpack and the overlying atmosphere and the greatest challenge faced currently is the model description of the air-snow grain interface. One group of models assume a disordered interface, DI, at the snow grain surface with liquid-like properties (e.g. Boxe and Saiz-Lopez, 2008; Thomas et al., 2011; Toyota et al., 2014; Murray et al., 2015). The DI is defined as a thin layer on the surface of the snow grain and is assumed to have the following characteristics; 1) DI reaction and partition rate constants are similar to those in the aqueous phase, e.g. Henry's Law ~~coefficient~~ coefficients are used to describe the partitioning between the two phases; 2) DI thickness ranges from <1 to a few hundreds nm based on observation (Bartels-Rausch et al., 2014) but is often set to an arbitrary value, e.g. 10 nm ~~(Thomas et al., 2011) and Murray et al., 2015;~~ (Thomas et al., 2011; Murray et al., 2015); and 3) ~~These models also assume~~ all (Toyota et al., 2014) or a fraction (Thomas et al., 2011; Murray et al., 2015) of the total solutes are located in the DI.

Another groups of models assume the interface between snow grain and surrounding air to be ice (e.g. Hutterli et al., 2003; Bock et al., 2016). The distribution of hydrogen peroxide, H_2O_2, and formaldehyde, HCHO, within the snowpack has been estimated using a physical air-snow and firn transfer model which included ~~a~~ temperature driven 'Air-Ice' uptake and release (Hutterli et al., 2003; McConnell et al., 1998). The ~~air-ice exchange~~ bulk concentration of H_2O_2 is ~~defined~~ determined by solid-state diffusion of H_2O_2 ~~whereas the exchange~~ in ice while the bulk concentration of HCHO is ~~described by linear adsorption isotherm of~~ determined by linear isotherm adsorption of HCHO on ice. A physical exchange model has been developed by Bock et al. (2016) to describe the concentration of NO_3^- in the skin layer at Dome C, East Antarctic Plateau. Bock et al. (2016) proposed the skin layer snow nitrate concentration at Dome C is determined by thermodynamic equilibrium ice solubility on the grain surface ~~(based on a parameterisation by Thibert et al., 1998)~~ followed by solid-state diffusion during winter. During summer the large increase in NO_3^- concentration in the skin layer snow is mainly ~~from~~ attributed to co-condensation of HNO_3 and H_2O~~(a kinetic process). The model of Bock et al. (2016)~~. However, Bock et al. (2016) model implies no loss of

NO_3^- due to sublimation, a process that has been suggested to be important in surface snow ~~dynamic (Röthlisberger et al., 2000).~~ dynamics (Röthlisberger et al., 2000).

Both types of models require tuning parameters used to fit the model output to a chosen set of observations. Some of these parameters do have a physical meaning yet the tuned values may not, for example the fraction of solute in the DI (Thomas et al., 2011) ~~,~~ or the ion partitioning coefficients (Hutterli and Röthlisberger, 1999)~~, or~~ . Whereas some may not have a strict physical meaning, for example the co-condensation ~~parameter (Bock et al., 2016),~~ related parameters were adjusted in Bock et al. (2016) model, one of their configurations (configuration 2-BC2) an empirical relationship between the co-condensation concentration, the partial pressure of nitric acid and water vapour while in another configuration (configuration 2-BC3) they varied the complementary error function when calculating the attribute from co-condensation to match the ~~model predictions with the field observations and hence are of limited predictive capacity~~modelled results to the observation. Any 'tuning' of a model to a specific set of observation may affect the confidence in projection of the model to other scenarios or conditions.

The aim of this paper is to develop a physical exchange model ~~from first principles~~ based on physical parameterisations and experimental data to describe the exchange of nitrate between the atmosphere and the skin layer of snow and minimising the number of tuning parameters~~and~~ . It is a first step towards a full snowpack model that would include deeper snow and other processes, such as wind pumping, molecular diffusion, and photochemistry. Two temperature dependent, multi-phase models, are developed to evaluate two different concepts to describe the interaction of nitrate between air and snow.

Model 1 is based on the hypothesis of the existence of a DI layer covering the entire snow grain above a threshold temperature, T_o (Sect. 3.1). Below T_o, the interface between snow grain and air is assumed to be 'Air-Ice', and the ~~grain surface~~ concentration of NO_3^- at the grain boundary is determined by non-equilibrium surface adsorption and co-condensation coupled with solid-state diffusion into the grain. Above T_o, the interface is assumed to be 'Air-DI' of which the NO_3^- concentration is defined by non-equilibrium solvation into the DI ~~followed by solid-state diffusion .~~ based on Henry's Law coefficient. This is similar to the approach taken by other models (e.g. Thomas et al., 2011; Toyota et al., 2014). The slight difference in Model 1 presented here to the previously developed models is that the DI is assumed 1) to have infinitesimal thickness; 2) to have a diffusion coefficient for nitrate with the same value as that measured in ice; and 3) to be interacting with the bulk.

Model 2 is based on the hypothesis of Domine et al. (2013), that liquid co-exists with ice above eutectic temperature, T_e. The liquid forms micropockets and ~~locate~~ is located in grooves at grain boundaries or triple junctions due to limited wettability of ice (Domine et al., 2013). Therefore, at all temperatures below melting the major interface between air and snow grain is assumed to be pure ice and the concentration of NO_3^- in ice is defined by non-equilibrium surface adsorption and co-condensation followed by solid-sate diffusion within the grain. Above T_e, the partitioning of

HNO_3 to the liquid micropockets is described by Henry's Law (Sect. 3.2). The total concentration of NO_3^- in the snow grain is the sum of the mass from both locations divided by the total volume of the snow grian.

Both models are validated with ~~data collected at~~ available observations from two sites in Antarctica that have very different atmospheric composition, temperatures and humidities; ~~The East Antarctic Plateau~~ One at Dome C ~~and secondly coastal Antarctica at Halley , where long-term atmospheric and meteorological observations are monitored at the Clean Air Sector Laboratory (CASLab) (Jones et al., 2008)~~on the East Antarctic Plateau and the other at Halley in coastal Antarctica, details described below.

2 Current Understanding of Physical Air-Snow Processes

Below we briefly review the current understanding of physical air-snow processes, which are relevant to nitrate. A more comprehensive discussion can be found in the recent review paper (Bartels-Rausch et al., 2014).

2.1 Surface Adsorption at the Air-Ice Interface

The probability of a gas molecule being adsorbed on a clean ice surface can be described by the dimensionless surface accommodation coefficient, α (Crowley et al., 2010). The adsorbed molecule can then be desorbed thermally or it can be dissociated and diffuse into the bulk and form a solid solution (Abbatt, 1997; Huthwelker et al., 2004; Cox et al., 2005). At a low partial pressure of HNO_3, the adsorption of HNO_3 on an ice surface can be expressed as the single-site Langmuir adsorption (Ullerstam et al., 2005b) with:

$$\mathrm{HNO_{3,(g)}} + \mathrm{S} \underset{k_{\mathrm{des}}}{\overset{k_{\mathrm{ads}}}{\rightleftharpoons}} \mathrm{HNO_{3,(ads)}} \tag{R1}$$

where $HNO_{3,(g)}$ and $HNO_{3,(ads)}$ are the gas-phase and surface adsorbed nitric acid. ~~[S] is the~~ and S is the surface site for adsorption. The concentration of surface ~~sites~~site, i.e. number of site available per unit volume of air~~and has a units of . It~~ is defined as ~~follows~~follow:

$$[\mathrm{S}] = (1-\theta)\, N_{max}\, \frac{\mathrm{A_{ice}}}{\mathrm{V_{air}}} \tag{1}$$

Here, θ is the fraction of ~~avilable~~ surface sites being occupied, N_{max} is the maximum number of surface sites with a unit of $\mathrm{molecule\,m_{ice}^{-2}}$, $\mathrm{A_{ice}}$ is the surface area of ice per unit volume of snowpack with a unit of $\mathrm{m_{ice}^2\,m_{snowpack}^{-3}}$, and $\mathrm{V_{air}}$ is the volume of air per unit volume of snowpack with a unit of $\mathrm{m_{air}^3\,m_{snowpack}^{-3}}$. Note that [$S$] has a units of $\mathrm{molecule\,m^{-3}}$. The adsorption coefficient, k_{ads} ,and desorption coefficient, k_{des}, in R1 are defined as

$$k_{\mathrm{ads}} = \frac{\alpha \overline{v}}{4} \frac{1}{N_{max}} \tag{2}$$

$$k_{\mathrm{des}} = \frac{k_{\mathrm{ads}}}{K_{\mathrm{eq}}} \tag{3}$$

Note that k_{ads} has a unit of $\mathrm{m^3\,molecule^{-1}\,s^{-1}}$ while the unit of k_{des} is $\mathrm{s^{-1}}$, $\overline{v}$ is the average gas-phase molecular speed and K_{eq} is the equilibrium constant for Langmuir adsorption on ice with a unit of $\mathrm{m^3\,molecule^{-1}}$. The value of K_{eq} for $\mathrm{HNO_3}$ is inversely correlated with temperature because the scavenging efficiency of $\mathrm{HNO_3}$ due to adsorption increases as temperature decreases. The parameterisations and values for the above variables used in this study are listed in App. A, Table A1. The value of the accommodation coefficient, α, is same as the experimental initial uptake coefficient, γ_0, if the time resolution of the laboratory experiments is high enough (Crowley et al., 2010). Fig. A1 shows the experimental initial uptake coefficients, γ_0, by various studies as a function of temperature. A comparison of different parameterisations of ~~α and~~ K_{eq} are shown in ~~App. A Fig. A1 and A2respectively~~Fig. A2.

2.2 Solid-State Diffusion

~~A solid solution of can be formed in ice due~~ Due to its solubility and diffusivity, $\mathrm{HNO_3}$ can form a solid solution in ice. The solid-state diffusion in natural snow ~~is~~ was found to be an important process for understanding the partitioning of highly soluble gases, including $\mathrm{HNO_3}$, between the atmosphere and snow ~~when interpreting the composition of environmental ice~~ (Bartels-Rausch et al., 2014). Thibert et al. (1998) derived a solid-state diffusion coefficient, k_{diff}, and a thermodynamic solubility of $\mathrm{HNO_3}$ in ice from sets of $\mathrm{HNO_3}$ concentration ~~-~~diffusion profiles obtained by exposing single ice crystal to diluted $\mathrm{HNO_3}$ at different temperatures for a period of days to weeks. However, Thibert et al. (1998) did not present the ~~the~~ kinetics of $\mathrm{HNO_3}$ uptake on ice and hence a characteristic time for equilibrium between air and ice could not be established. A diffusion-like behaviour has been observed from flow-tube studies for trace gas uptake onto ice (e.g. Abbatt, 1997; Huthwelker et al., 2004; Cox et al., 2005) suggesting the solid-state diffusion of nitrate molecules can occur concurrently with surface adsorption (R1), such that

$$\mathrm{HNO_{3,(ads)}} \overset{k_{\mathrm{diff}}}{\rightleftarrows} \mathrm{HNO_{3,(ice)}} \tag{R2}$$

where $\mathrm{HNO_{3,(ice)}}$ is the nitric acid incorporated into the ice matrix~~, occurs with R1~~.

2.3 Coexistence of Liquid Solution with Ice

Liquid aqueous solution coexists with ice in the presence of soluble impurities, such as sea salt and acids. The liquid exist down to the eutectic temperature defined by the composition and solubility of the impurities in the ice. Cho et al. (2002) parameterised the liquid water fraction, $\phi_{\mathrm{H_2O}}(T)$, as a function of total ionic concentration of impurities, $\mathrm{Ion_{tot}}$,and temperature as follows:

$$\phi_{\mathrm{H_2O}}(T) = \frac{\overline{m}_{\mathrm{H_2O}} R T_f}{1000 \Delta H_f^0} \left(\frac{T}{T_f - T}\right) \Phi_{\mathrm{bulk}}^{\mathrm{aq}} \left[\mathrm{Ion_{tot\,(bulk)}}\right] \tag{4}$$

where $\phi_{\mathrm{H_2O}}(T)$ has a units of $\mathrm{m^3_{liquid}\,m^{-3}_{liquid+solid}}$, $\overline{m}_{\mathrm{H_2O}}$ is the molecular weight of water, R is the ideal gas constant, T_f is the freezing temperature of pure water in K, ΔH_f^0 is the enthalpy of

fusion in $\mathrm{J\,mol^{-1}}$, $\Phi^{\mathrm{aq}}_{\mathrm{bulk}}$ is the fraction of the total solute in the aqueous phase and $[\mathrm{Ion_{tot,\,bulk}}]$ is the total ionic concentration in the melted sample. There are different hypothesises ~~on~~ regarding the location of the liquid solution. Most studies assume the liquid solution forms a thin layer covering the whole grain surface (e.g. Kuo et al., 2011) while Domine et al. (2013) suggested the liquid is located in grooves at grain boundaries and triple junctions. The arguments of the latter study were 1) the ionic concentration is low in natural snow that only small amount of liquid can be formed; and 2) the wettability of liquid water on ice is imperfect, preventing the liquid drop from spreading out across the solid surface. The volume of liquid is small relative to the ice grain and if spread uniformly across the ice grain the thickness would be less than ~~a~~ the diameter of the $\mathrm{H_2O}$ molecule which is unrealistic.

The partitioning of ~~trace~~ atmospheric acidic gases between air and the liquid fraction of snow can be described by Henry's law using the effective dimensionless Henry's law coefficient, $k^{\mathrm{eff}}_{\mathrm{H}}$, according to Sander (1999)

$$k^{\mathrm{eff}}_{\mathrm{H}} = k^{\mathrm{cc}}_{\mathrm{H}} \frac{\mathrm{K_a}}{[\mathrm{H^+_{(aq)}}]} \tag{5}$$

where $k^{\mathrm{cc}}_{\mathrm{H}}$ is the dimensionless temperature dependent Henry's Law coefficient (See App. A), $\mathrm{K_a}$ is the acid dissociation constant and $[\mathrm{H^+_{(aq)}}]$ is the concentration of hydrogen ions. Fig. A3 shows the temperature and pH dependence of $k^{\mathrm{eff}}_{\mathrm{H}}$. At a given ~~pH~~temperature, $k^{\mathrm{eff}}_{\mathrm{H}}$ ~~varies by a 2 orders of magnitude between -40°C and 0°C~~increases by an order of magnitude (Fig. A3 A) between pH 5 and 6.5, the typical range of pH in natural snow (Udisti et al., 2004). While at a given ~~temperature~~pH, $k^{\mathrm{eff}}_{\mathrm{H}}$ ~~varies within one order of magnitude (See~~ decreases by 2 orders of magnitude between -40°C and 0°C (Fig. A3 ~~), for typical pH value of natural surface snow (5 - 6.5, Udisti et al., 2004)~~B).

3 Modelling Approach

The ~~model constraints are~~ models are constrained by the observed atmospheric concentration of $\mathrm{HNO_3}$, air temperature, skin layer temperature, atmospheric pressure and humidity. The loss or gain in the atmospheric ~~concentration of~~ $\mathrm{HNO_3}$ due to the mass exchange between air and snow are included implicitly by constraining the models with the observed atmospheric concentration of $\mathrm{HNO_3}$. The aim of this paper is to focus on the exchange mechanisms of $\mathrm{HNO_3}$ between air and snow to predict the concentration of nitrate in snow, limited to the skin layer, as a first step towards a full snowpack model. The following assumptions were made, 1) homogenous physical properties across the skin layer, such as snow density and specific surface area~~(SSA)~~, SSA. 2) the concentration of $\mathrm{HNO_3}$ in SIA is the same as the overlying atmosphere due to a short gas-phase diffusion characteristic time scale of $\sim 10^0$ s (Table 1).

For simplicity, the snow grain is assumed to be a radially symmetrical sphere with ~~a~~ radius, $\mathrm{R_{eff}}$, which is estimated from the SSA as the follows:

$$\mathrm{R_{eff}} = \frac{3}{\rho_{\mathrm{ice}}\,\mathrm{SSA}} \tag{6}$$

where ~~ρ_{ice}~~ ρ_{ice} is the density of ice. In addition, the grain morphology is also assumed to be constant ~~,~~ with time, with the exception of co-condensation Eq. 9 & 10, i.e. snow metamorphism is not taken into account.

3.1 Model 1 - Surface Adsorption/Solvation & Solid Diffusion

In Model 1, the uptake of $\mathrm{HNO_3}$ is treated as a two-step process consisting of interfacial mass transport across the air-snow grain boundary and subsequent diffusion into the bulk, a similar approach as taken by Bock et al. (2016). Below a threshold temperature, ~~T_0, (~~T_o, (an experimental based value, details in Sect. 3.1.1 & Fig. 1a) the ~~concentration of nitrate at the snow grain~~ snow grain boundary is assumed to be 'Air-Ice' of which the concentration of the boundary is defined by the combination of adsorption and co-condensation ~~. Above T_0~~ on ice. Above T_o, the snow grain boundary ~~concentration~~ is assumed to be 'Air-DI', of which the concentration of the boundary is defined by solvation governed by Henry's law into the disordered interface, DI, (~~See~~ Details in Sect. 3.1.2 & Fig. 1b).

A DI on pure ice has been detected between 238 and 270 K depending on the measurement technique (Domine et al., 2013 and references therein). The threshold temperature, T_o, for the work described here is set to the lower end of the range ~~(~~238 K~~). The difference in concentration of nitrate between the grain boundary and its centre drives the transport of within the grain, which can be characterised by the~~ . Model uncertainties due to the uncertainties in T_o are evaluated in a sensitivity study further below (Sect. 6.5).

The physical properties of the DI, such as the layer thickness, partitioning coefficient, diffusivity etc., are still poorly understood. The laboratory measurements of thickness of DI of pure ice range from a monolayer of water to around a few hundreds of nm (Bartels-Rausch et al., 2014) also depending on the measuring techniques and temperature. Thur there is no physical parameterisation available to estimate the thickness of DI as a function of temperature and/or concentration within the bulk. There are no values available for the air-DI partitioning and the diffusivity of the DI neither, therefore, for the DI in Model 1 has the following is assumed: 1) the partitioning between air and the DI is governed by Henry's law; 2) the DI is interacting with the bulk ice, which the solvated nitrate molecules are allowed to diffused into the bulk ice, the rate of the transport is limited by the diffusivity of solid ice; and 3) the DI has an infinitesimal thickness and the concentration in the DI is acting as the boundary condition of the solid-state diffusion ~~of (~~into the snow grain (See Sect. 3.1.3). Note that besides adopting Henry's law coefficient as the partitioning coefficient between air and DI, the other assumptions made here for the DI is different from the assumptions made by previous

models (e.g. Thomas et al., 2011; Toyota et al., 2014) that often assume the DI has a certain arbitrary thickness and isolated from the bulk ice.

3.1.1 ~~Ambient Temperature $\leq$~~ $T \leq$ 238 K: Non-Equilibrium Surface Adsorption & Co-condensation

At a temperature below ~~T_0~~ T_o = 238 K the interface between air and snow grain is assumed to be pure ice. The concentration of nitrate at the grain boundary, $[\mathrm{HNO_{3\,(surf)}}]$, is determined by a combination of non-equilibrium kinetic adsorption and co-condensation:

$$[\mathrm{HNO_{3\,(surf)}}] = [\mathrm{HNO_{3\,(ads)}}] + [\mathrm{HNO_{3\,(cc)}}] \qquad \text{if} \quad T \leq 238\mathrm{K} \tag{7}$$

where $[\mathrm{HNO_{3\,(ads)}}]$ is the concentration contributed by the sum of surface adsorption and desorption ~~(Eq. 8),~~ and $[\mathrm{HNO_{3\,(cc)}}]$ is the concentration contributed by co-condensation or co-sublimation~~(Eq. 9).~~

. This configuration but without the contribution by co-condensation is referred as 'Model 1 - BCice' hereon. The net rate of adsorption can be described as $\frac{d[\mathrm{HNO_{3\,(ads)}}]}{dt} = k_{\mathrm{ads}}[\mathrm{HNO_{3\,(g)}}][\mathrm{S}] - k_{\mathrm{des}}[\mathrm{HNO_{3\,(ads)}}]$. Substituting k_{des} with Eq. (3), the net adsorption rate is expressed as

$$\frac{d[\mathrm{HNO_{3\,(ads)}}]}{dt} = k_{\mathrm{ads}}\left([\mathrm{HNO_{3\,(g)}}][\mathrm{S}] - \frac{[\mathrm{HNO_{3\,(ads)}}]}{K_{\mathrm{eq}}}\right) \tag{8}$$

A non-equilibrium kinetic approach is taken instead of saturation or equilibrium adsorption for two main reasons: ~~Firstly~~firstly, Ullerstam et al. (2005b) have shown that for partial pressures of $\mathrm{HNO_3}$ lower than 10^{-5} Pa the ice surface is not entirely covered with $\mathrm{HNO_3}$ and therefore undersaturated. The annual average atmospheric partial pressure of $\mathrm{HNO_3}$ recorded at Dome C is $\sim 10^{-6}$ Pa (Traversi et al., 2014) and is $\sim 10^{-7}$ Pa at Halley (Jones et al., 2008), hence, the ice surface is unlikely to be saturated with $\mathrm{HNO_3}$. Secondly, natural snowpacks are constantly undergoing sublimation and condensation of $\mathrm{H_2O}$, especially at the skin layer, due to temperature gradient over a range of timescales from a fraction of seconds to days and seasons (Bartels-Rausch et al., 2014). Pinzer et al. (2012) observed up to 60% of the total ice mass redistributed under a constant temperature gradient of 50 $\mathrm{K\,m^{-1}}$ over a 12 hour period. Field observations (Frey et al., 2013) and the results from a heat transfer model (Hutterli et al., 2003) at Dome C in summer show ~~absolute~~ temperature gradients of 71 $\mathrm{K\,m^{-1}}$ across the top 2 cm and 130 $\mathrm{K\,m^{-1}}$ across the top 4 mm of the snowpack, respectively. At Halley, the modelled summer ~~absolute~~ temperature gradient in the top cm of snow is about 41 $\mathrm{K\,m^{-1}}$. Therefore, the dynamic $\mathrm{H_2O}$ exchange and redistribution at the snow grain surface prevent the equilibrium of adsorption from being reached and require a kinetic approach.

The temperature gradient and relative humidity gradient between the surface of the snowpack and the skin layer create a gradient in water vapour pressure, which drives condensation or sublimation of ice, depending on the sign of the gradient. Uptake of $\mathrm{HNO_3}$ molecules to growing ice is known as co-

condensation. The surface concentration of NO_3^- contributed by co-condensation or co-sublimation, $[HNO_{3\,(cc)}]$, is given by

$$[\mathrm{HNO_{3(cc)}}] = X_{\mathrm{HNO_3}} \frac{\rho_{ice}\, N_A}{\overline{m}_{\mathrm{H_2O}}} \frac{\Delta t}{\mathrm{V_{grain}}} \frac{d\mathrm{V}}{dt} \tag{9}$$

where $\mathrm{X_{HNO_3}}$ is the mole fraction of HNO_3 condensed along with water vapour ($\mathrm{X_{HNO_3}} = 10^{-3.2}\, P_{\mathrm{HNO_3}}^{0.56}$, Ullerstam and Abbatt, 2005a), ρ_{ice} is the density of ice (in $\mathrm{kg\,m^{-3}}$), N_A is Avogadro's constant (6.022×10^{23} $\mathrm{molecule\,mol^{-1}}$) and Δt is the model time step. The rate of volume change of snow grain, $\frac{dV}{dt}$, is specified by the growth law ~~by described (Flanner and Zender, 2006)~~ described by Flanner and Zender (2006)

$$\frac{d\mathrm{V}}{dt} = \frac{4\,\pi\,\mathrm{R_{eff}^2}}{\rho_{ice}} D_v \left(\frac{d\,\rho_v}{d\,x}\right)_{x=r} \tag{10}$$

where D_v is the diffusivity of water vapour in air and $\frac{d\rho_v}{dx}$ is the local water vapour density gradient, i.e. between air away from the snow grain and the air near the grain surface. However, to the author's knowledge there are no observations reported and the calculation of water vapour density at these microscopic scales is computational costly as it would require 3-D modelling of the metamorphism of the snow grain. For simplicity, the macroscopic (few mm) water vapour gradient across the skin layer was used to estimate the rate of volume change of snow grain due to condensation or sublimation, i.e. $\left(\frac{d\rho_v}{dx}\right)_{x=r}$ in Eq. 10 is replaced by $\left(\frac{d\rho_v}{dz}\right)_{z=4\mathrm{mm}}$. The water vapour density, ρ_v, can be calculated as follows:

$$\rho_v = \frac{P_{sat}\,\mathrm{RH}}{100\,R_v\,T} \tag{11}$$

where P_{sat} is the saturated vapour pressure (Pa), RH is the relative humidity (%), R_v is the gas constant ($\mathrm{J\,kg^{-1}\,K^{-1}}$) and T is temperature (K). There are no measurements of fine resolution of vertical snow profile of RH and temperature available, therefore, RH within the snowpack was assumed to be 100% and the temperature of the skin layer is estimated using a heat transfer temperature model based on the heat diffusion equation (Hutterli et al., 2003):

$$\frac{\partial T}{\partial t} = \frac{\partial}{\partial z} k_w(z) \frac{\partial T}{\partial z} \tag{12}$$

where T is the temperature, t is time, k_w is the thermal conductivity (App. A, Table A1) of snowpack and z is the depth.

3.1.2 ~~Ambient Temperature >~~ *T* > 238 K: Non-Equilibrium Solvation

~~At temperature above T_0~~

At temperatures above T_0 = 238 K the interface between air and ~~snow grain surface~~ the entire surface of the snow grain is assumed to be a DI. ~~The DI is assumed to be covering the entire grain surface and the partitioning into the DI based on Henry's law. The grain boundary concentration is~~

~~determined by non-equilibrium solvation into the DI such that~~

$$[\mathrm{HNO_{3\,(surf)}}] = [\mathrm{HNO_{3\,(DI)}}] \qquad \text{if} \quad T > 238\mathrm{K} \tag{13}$$

The DI is also assumed to be out of equilibrium with the surrounding air ~~for similar reasons as discussed above (~~as the exchange of water molecules at the surface of the snow grain is expected to be rapid that the surface is redistributed before equilibrium is reached (Details in Sect. 3.1.1). The ~~grain boundary concentration~~ concentration of the DI is then defined by the following equation:

$$\frac{d[\mathrm{HNO_{3\,(DI)}}]}{dt} = k_{\mathrm{mt}} \left([\mathrm{HNO_{3\,(g)}}] - \frac{[\mathrm{HNO_{3\,(DI)}}]}{k_{\mathrm{H}}^{\mathrm{eff}}} \right) \tag{14}$$

The mass-transfer coefficient, k_{mt}, is defined as $k_{\mathrm{mt}} = \left(\frac{\mathrm{R_{eff}}^2}{3\,D_g} + \frac{4\,\mathrm{R_{eff}}}{3\,\overline{v}\,\alpha} \right)^{-1}$, where D_g is the gas-phase diffusivity (Sander, 1999). Note that in this model the ~~DI is treated as the boundary between the air and bulk ice. The~~ concentration of the DI is used as the outermost boundary condition for ~~solid- state~~ solid-state diffusion within the grain ~~, therefore, the DI has no thickness~~(See Sect. 3.1.3) and the transfer of $\mathrm{NO_3^-}$ into the bulk is limited by the concentration gradient across the snow grain and the diffusivity in ice.

3.1.3 Solid-State Diffusion

The concentration gradient between the grain boundary and its centre drives solid state diffusion of nitrate within the bulk ice. The ~~concentration at the grain boundary is defined by surface adsorption and co-condensation at temperatures below T_0 or solvation into the DI at temperatures above T_0, discussed above. The~~ $\mathrm{NO_3^-}$ concentration profile within the snow grain can be found by solving the following partial differential equation

$$\frac{\partial[\mathrm{NO_3^-}](r)}{\partial t} \frac{\partial U(r)}{\partial t} = k_{\mathrm{diff}} \left(\frac{2}{r} \frac{\partial[\mathrm{NO_3^-}](r)}{\partial r} + \frac{\partial^2[\mathrm{NO_3^-}](r)}{\partial r^2} \frac{\partial^2 U(r)}{\partial r^2} \right) \tag{15}$$

where ~~$[\mathrm{NO_3^-}](r)$ is the local concentration in the~~ $U(r)$ is the concentration at distance r ~~concentritic layer of the ice sphere~~ from the centre of the snow grain and k_{diff} is the ~~solid state diffusion coefficientfor ice. The~~ solid-state diffusion coefficient, which is assumed to be homogeneous across the snow grain. The nitrate concentration at the centre is set to $U(0) = 0$ and at the grain boundary $U(R_{\mathrm{eff}}) = [\mathrm{HNO_{3\,(surf)}}]$, which is defined by surface adsorption and co-condensation at temperatures below T_o (Eq. 7) or by solvation into the infinitesimal DI at temperature above T_o (Eq. 13).

The typical length-scale, <x>, a molecule diffuses in a given time, t, can be described by the root-mean square displacement, <x> = $\sqrt{6\,t k_{\mathrm{diff}}}$. The typical length-scale, <x>, is 1.5 and 5.5 μm at Dome C (Sect. 4.1) and Halley (Sect. 4.2), respectively, during a model time step of Δt = 10 min. The effective radius of the snow grain at Dome C and Halley is estimated to be between 30-130 µm (Fig. A4). To optimise the performance and computational cost of the models ~~,~~ the snow grain is divided into N = 85 evenly spread concentric shells (i.e. ~~r = 1~~ $r = 0, n\Delta r$ with $n = 1, 2, \ldots, N$ and

$R_{\text{eff}} = N\Delta r$), ~~2, 3, ..., 85 with 85being the outermost shell)were used to represent the snow grain,~~ such that the thickness of the concentric shell is less than the average root-mean square displacement.

The diffusion equation is solved with the Crank-Nicolson scheme (Press et al., 1996) and the bulk concentration of NO_3^- in the ice grain, $[NO^-_{3\,(\text{bulk})}]$, is the sum of the number of NO_3^- molecules in each layer divided by the volume of the whole grain, expressed as

$$[NO^-_{3\,(\text{bulk})}] = \frac{\sum [NO_3^-](r)\,V(r)}{\sum V(r)} \frac{\sum [NO_3^-](n)\,V(n)}{\sum V(n)} \tag{16}$$

where ~~$V(r)$ is the volume of the r^{th} layer and $\sum V(r)$ is the total~~ $[NO_3^-](n)$ is the concentration of nitrate in the n^{th} layer that is calculated by linear interpolating values of $U(r-1)$ and $U(r)$, $V(n)$ is the volume of the n^{th} layer and $\sum V(n)$ is the total volume of the grain, V_{grain}~~, and (r) is the concentration of nitrate in the r^{th} layer~~.

3.2 Model 2 - Non-Equilibrium Kinetic Adsorption & Solid Diffusion and Equilibrium Air - Liquid Micropocket

Model 2 is based on the hypothesis that the major air-snow grain interface is pure ice at all temperatures below ~~the melting~~ melting temperature, T_m, and that liquid coexists with ice when the temperature is above the eutectic temperature, T_e (Fig. 2). The liquid water is assumed to be located in grooves at grain boundaries or triple junctions between grains and in the form of micropockets. This assumption implies that the grain surface area being covered by liquid water is negligible. The bulk concentration of NO_3^- in Model 2 is defined as follows:

$$[NO^-_{3\,(\text{bulk})}] = \begin{cases} \frac{\sum [NO_3^-](r)\,V(r)}{V_{\text{grain}}} & \text{if} \quad T < T_e. \\ \frac{\sum [NO_3^-](r)\,V(r)}{V_{\text{grain}}} + \phi_{H_2O}\, k_H^{\text{eff}}\, [HNO_{3\,(g)}] & \text{if} \quad T_e \le T < T_m. \end{cases} \tag{17}$$

~~At~~ The term '$\frac{\sum [NO_3^-](r)\,V(r)}{V_{\text{grain}}}$' in Eq. 17 is representing the nitrate concentration in the ice-phase and is applied to all temperatures below the melting temperature, T_m. At $T < T_m$, HNO_3 can be adsorbed/desorbed and co-condensed/co-sublimated from the ~~surface as~~ ice surface as was the case in Model 1 when $T < T_e$ (Sect. 3.1.1). The adsorbed and co-condensed molecules on the ~~grain~~ ice surface then diffuse into or out of the bulk ice depending on the concentration gradient of nitrate ~~as~~ anion as was the case in Model 1 (Sect. 3.1.3). ~~Above T_e~~ The nitrate in the snow grain contributed by these processes is referred to as the ice-phase nitrate.

The term '$\phi_{H_2O}\, k_H^{\text{eff}}\, [HNO_{3\,(g)}]$' in Eq. 17 is representing the nitrate concentration in the liquid-phase when $T \ge T_e$. At $T \ge T_e$, liquid co-exists with ice, and ~~its volume~~ the bulk mass of NO_3^- is attributed from NO_3^- located both within the ice and in the liquid micropocket. The volume of liquid can be calculated from the liquid water fraction, ϕ_{H_2O} (Eq. 4). The ~~term '$\phi_{H_2O}\, k_H^{\text{eff}}\, [HNO_{3\,(g)}]$' in Eq. 17 is the bulk concentration of nitrate contributed from the solvation of nitric acid in the liquid micropockets. The~~ liquid in the micropocket is assumed to be ideal and the partitioning between air

and liquid ~~micropockets~~ micropocket is described by Henry's Law ~~, with the effective Henry's Law coefficient, k_H^{eff}, as the partitioning coefficient. An instantaneous equilibrium is assumed because~~(Eq. 5). This implies instantaneous equilibrium between air and liquid micropocket, and is justified because; 1) the volume of the liquid solution is small ~~(~~which up to $10^{-7} - 10^{-6}$% of the total volume of the ice grain ~~,~~ (as discussed below); 2) HNO_3 is strongly soluble in water; 3) the characteristic time of the interfacial mass transport across a liquid surface of a droplet with 70 μm diameter is only $\sim 10^{-7}$ s (Table 1); and 4) the ~~diffusion rate~~ diffusivity of HNO_3 is faster in ~~liquid (~~liquid-phase (9.78×10^{-10} $m^2\,s^{-1}$ at 0°C, ~~diffusion of is 9.78×10^{-10} in liquid,~~ Yuan-Hui and Gregory, 1974) than in ice (3.8×10^{-14} $m^2\,s^{-1}$ at 0°C~~, diffusion of is 3.8×10^{-14} in ice~~). The characteristic time of liquid-phase diffusion within a 70 μm diameter water droplet is $\sim 10^0$ s (Table 1).

Both the values of pH and Φ_{bulk}^{aq} (in Eq. 4) are updated at each model time step with values from the previous time step. At Dome C, the major anion in melted snow is NO_3^- (e.g. Udisti et al., 2004). Therefore, it is assumed that nitrate and hydrogen ions are the only ions present in the skin layer snow, i.e. $[\mathrm{Ion}_{\mathrm{tot\,(bulk)}}]$ = 2×$[NO_3^-]$ in Eq. 4, and the eutectic temperature of ~~the~~ a H_2O-HNO_3 system of 230.64 K (Beyer et al., 2002) ~~are~~ is chosen as the threshold temperature for the existence of micropockets. In contrast, at Halley snowpack ion chemistry is dominated by NaCl (Wolff et al., 2008), contributing ~~85~~70% to the total ion concentration in the 2004-05 Halley data set, due to the proximity of sea ice and open ocean. ~~For~~ Surface snow at Halley also contains a significant amount of sulphate ion, SO_4^-, attributed from sea salt sulphate and sulphuric acid, together contributing ~ 20% of the total ion concentration. However, for simplicity, the only anions included in the calculation of ϕ_{H_2O} at Halley are NO_3^- and Cl^-, such that $[\mathrm{Ion}_{\mathrm{tot\,(bulk)}}]$ = 2×($[Cl^-]$ + $[NO_3^-]$) in Eq. 4 and the value of T_e used is that for a H_2O-NaCl system of 251.95 K (Akinfiev et al., 2001).

3.3 Model BC1 by Bock et al. (2016)

Previously Bock et al. (2016) developed a model for air and ice exchange of nitrate in surface snow assuming only air-ice interaction, which is in equilibrium with the surrounding air. They defined the concentration of nitrate (Bock et al., 2016, Configuration 2 - BC1) in the outermost layer of the snow grain by the thermodynamic equilibrium solubility parameterisation by Thibert et al. (1998):

$$[NO_3^-](n = N) = 2.37 \times 10^{-12} \exp\left(\frac{3532.2}{T}\right) P_{HNO_3}^{1/2.3} \frac{\rho_{ice} N_A}{\bar{m}_{H_2O}} \quad (18)$$

where N is the number of concentric shells in the snow grain, T is the snow temperature (K), P_{HNO_3} is the partial pressure of HNO_3 (Pa) and $\bar{m}_{H_2O}$ is the molar mass of H_2O. They concluded that the concentration of nitrate in surface snow at Dome C during winter is mainly govern by thermodynamic equilibrium solubility coupled to solid-state diffusion.

The configuration after Bock et al. (2016), where the concentration of nitrate in snow grain is defined by equilibrium solubility at the air-ice interface coupled to solid-state diffusion (referred as 'Bock - BC1' from hereon, of which BC stand for boundary condition) is compared with the

non-equilibrium adsorption coupled to solid-state diffusion configuration presented in this paper ('Model 1 - BCice', Sect. 3.1.1). Note that the co-condensation was excluded in these model runs for a direct comparison between the two different approaches. The two configurations are analysed and discussed in Sect. 6.1 based on data collection during winter at Dome C and Halley.

4 Model Validation

Model calculations are constrained and validated with existing ~~observation~~ observations of atmospheric nitrate ~~,~~ and meteorology and with skin layer snow NO_3^- concentration ~~and meteorological data at~~ from Dome C and Halley. Below a brief summary of the available data is given.

4.1 Observation at Dome C

Dome C is characterised by the following: 1) temperatures are below ~~freezing~~ the freezing point year round, and no snow melt occurs, with an annual mean of $-52°C$~~and a~~ , maximum of $-17°C$ in summer (mid November till end of January) and minimum temperature of $-80°C$ in winter (April to mid September) ~~(e.g. Argentini et al., 2014).~~ as shown in Fig. 3 A (Erbland et al., 2013). The diurnal temperature variation is $\sim$10 K in summer, spring (mid September until mid November) and autumn (February to March). 2) the air-snow chemistry of reactive nitrogen is relatively simple due to the remoteness of the site. In particular, concentrations of sea salt and other particles that ~~scavenge~~ may scavenge atmospheric HNO_3 ~~in the air~~ are low on the East Antarctica Plateau (Legrand et al., 2016). Hence, the main atmospheric nitrate is gaseous HNO_3 that dissolves in and/or adsorbs onto snow grains (Traversi et al., 2014). 3) Furthermore, a low snow accumulation rate of 27 $kg\,m^{-2}\,yr^{-1}$ (Röthlisberger et al., 2000) ~~allows~~ leads to significant post-depositional processing of nitrate driven by photolysis before the surface snow is buried by new snowfall (e.g. Röthlisberger et al., 2000; Frey et al., 2009).

Observations of skin layer snow nitrate concentration, atmospheric nitrate concentration, temperature, and pressure were carried out previously at Dome C during January 2009 to 2010 ~~at Dome C~~ (Erbland et al., 2013) and are shown in Fig. 3. The snow samples were collected from the 'skin layer' snow, the top 4 ± 2 mm of the snowpack, approximately every 3 days (Erbland et al., 2013). The skin layer was assumed to be spatially heterogeneous with an uncertainty in thickness of about 20% due to the softness of the uppermost layer and sampling by different people. The nitrate concentration in the melted sample was measured by ion chromatography ~~(IC)~~ (Erbland et al., 2013).

The concentration of atmospheric nitrate, i.e. the sum of atmospheric particulate nitrate ($p-NO_3^-$) and the concentration of gaseous nitric acid (HNO_3), was collected on glass fibre filters ~~by~~ with a high volume air sampler (HVAS) as described in Morin et al. (2008). Erbland et al. (2013) stated that the concentration of ~~particulate~~ atmospheric nitrate shows good agreement with HNO_3 gas-phase concentration measured by denuder tubes at Dome C over the same time period, therefore we equate

the observed atmospheric nitrate with gaseous HNO_3. The filter was positioned approximately 1 m above the snow surface and changed weekly. The atmospheric boundary layer is assumed to be well mixed so that the atmospheric nitrate at the snowpack surface would be the same at 1 m. The characteristic transport time of HNO_3 from the snowpack surface to the skin layer (4 mm) is on the order of 10^0 s, which is much shorter than the temporal resolution of the model (10 min, Table 1). Therefore, the concentration of ~~in the~~ gaseous HNO_3 in the open pore space of the skin layer was assumed to be the same as in the air above the snow. The ~~maximum concentration of atmospheric~~ concentration of ~~167 was observed during the summer period, while the minimum concentration of 1.2 was recorded during the autumn and early winter period.~~ gaseous HNO_3 was more than 2 orders of magnitude higher in the summer than in autumn/ early winter (Fig. 3 B).

Continuous meteorological observation and snow science are carried out at Dome C under the 'Routine Meteorological Observations' of the Concordia Project by the Italian National Antarctic Research Programme, PNRA, and the French Polar Institute, IPEV (http://www.climantartide.it). Temperature and humidity were measured at 10 s resolution. Both the temperature and relative humidity were measured at 1.6 m above the snow surface with a platinum resistance thermometer (VAISALA PT100 DTS12) with a precision of $\pm$ 0.13 °C at -15 °C, and the humidity sensor (HUMICAP, VAISALA) had a precision of $\pm$ 2 %. Based on the assumption of a well mixed boundary layer, the RH above the snowpack surface was assumed to be the same as that at 1.6 m. Atmospheric nitrate concentrations and meteorological data used as model input have been linearly interpolated to 10 minute resolution.

4.2 Observation at Halley

Halley ~~, in coastal Antarctica,~~ is at a similar latitude as Dome C but ~~at sea level~~ in coastal Antarctica ~~, as opposed to the Antarctic Plateau,~~ at sea level and with very different geographic features. Halley is on the Brunt Ice Shelf and is close to the Weddell Sea in three directions. Hence the temperature, relative humidity, and concentration of atmospheric aerosol are much larger at Halley than Dome C. The average surface temperature in summer days is around $-10°C$ and below $-20°C$ in the winter. Occasionally, the temperature can rise above $0°C$ (surface melt is possible) or drop to $-55°C$ (See Fig. 4 A). The annual mean snow accumulation rate at Halley is ~~much~~ 480 $kg\,m^{-2}\,yr^{-1}$ (Wolff et al., 2008), about one order of magnitude larger than at Dome C ~~, which has an average of 480 (Wolff et al., 2008),~~ and therefore limiting post-depositional processes relative to Dome C.

Meteorological and chemical data were collected at Halley under the CHABLIS (Chemistry of the Antarctic Boundary Layer and the Interface with Snow) campaign at the Clean Air Sector Laboratory (CASLab), (details in ~~Jones et al. (2008, 2011)).~~ Jones et al., 2008, 2011). The site description and data given in details elsewhere (Jones et al., 2008), below is a brief description. Measurement of atmospheric concentration of HNO_3 were carried out at weekly resolution using annular denuders (URG corporation) mounted 7-8 m above the snow surface with a collection efficiency of 91%

~~(Jones et al., 2008).~~ (Fig. 4 B). The atmospheric boundary layer is assumed to be well-mixed so that the nitric acid concentration at the snowpack surface would be the same as at 7-8 m. Surface snow (the top 10 to 25 mm) was collected on a daily basis and the samples were analysed using ion chromatography (~~IC~~Fig. 4 B). Bulk concentrations of the major anions and cations were measured, including Cl^-, SO_4^{2-} and NO_3^- (Wolff et al., 2008). The concentrations were interpolated to the 10 minutes model resolution.

Other meteorological data included 10 minute averages of air temperature by Aspirated PRT, RH by Humidity probe (Vaisala Corp) and wind speed and direction by Propeller vane. All sensors were at 1 m above the snow surface~~(Fig. 4).~~. All values were linearly interpolated to the model time step of 10 min.

4.3 Other Model Inputs

There are no available pH measurements of the snowpack, therefore, the pH of the DI in Model 1 and the initial pH in Model 2 is assumed to be 5.6 ~~(Udisti et al., 2004)~~ (Udisti et al., 2004, based on the pH of the completely melted samp both Dome C and Halley. There are no ~~measurement~~ measurements of SSA recorded during 2009-2010 for skin layer snow. The SSA and effective grain radius in this study are estimated based on ~~observation~~ observations at Dome C from 2012 to 2015 by Picard et al. (2016), as shown in Fig. A4~~,~~ ~~solid line. No~~ . To the author's knowledge there are no observations of SSA are available for Halley. Therefore the observations of SSA from Dome C were adjusted taking into account the shorter cold period, which tends to have a larger SSA (Fig. A4, dashed line).

4.4 Statistical Analysis

Three-day running means are calculated from all model outputs to better match the time resolution of the snow observations. The performance of the models is assessed by the coefficient of variation of RMSE, $\mathrm{C_v(RMSE)}$, as a goodness of fit. The $\mathrm{C_v(RMSE)}$ is defined as

$$\mathrm{C_v(RMSE)} = \frac{\sqrt{\sum_{t=1}^{n}(obs(t) - model(t))^2 / n}}{\overline{obs}} \tag{19}$$

where $obs(t)$ and $model(t)$ are the observed value and modelled value at time t respectively, n is the number of observations, and $\overline{obs}$ is the observation mean.

5 Results

5.1 Dome C

The predicted concentration of nitrate in skin layer snow for Model 1 and Model 2 in Dome C (Fig. 5 and Table 2) are discussed by season - Winter to Spring (April - Mid November) and Summer (Mid November - January).

5.1.1 Winter to Spring

The average temperature ($\pm 1\sigma$) at Dome C between late autumn to late spring in 2009 is 213.7 ($\pm$7.9) K (Fig. 3 ~~a~~A), which is below the threshold temperature, ~~T_0~~T_e, for detection of DI layer (set at 238 K, purple shaded area in Fig. 5 A) for Model 1 and below the eutectic temperature, T_e, for a H_2O-HNO_3 mixture (230 K, yellow shaded area in Fig. 5 B) for Model 2. Therefore, in winter, the skin layer concentration of nitrate ~~described well~~ is well described by non-equilibrium kinetic surface adsorption and co-condensation coupled to solid-state diffusion within the snow grain in both models. The models combine both processes and ~~agreed~~ agree very well with the observations of nitrate (Fig. 5 ~~a~~A & B) with a $C_v(\mathrm{RMSE}) = 0.73$ (Table 2). Both models captured the small peak from mid April to early May and another peak from mid to end of August then a steady increase from middle September till the ~~end of October~~beginning of November, except for the peak in late February.

~~Below we compare our 'Kinetic approach' (a 'non-equilibrium surface adsorption followed by solid diffusion' configuration) with the 'Equilibrium approach' suggested by Bock et al. (2016, Configuration 2 - BC1) in estimating skin layer in the winter period (~~The results from 'Bock-BC1' and 'Model 1 - BCice' are shown in Fig. 6a~~). The grain surface concentration, , for the 'Equilibrium' approach is determined by parameterisation from Thibert et al. (1998):~~

$$[\mathrm{HNO_{3\,(surf)}}] = 2.37 \times 10^{-12} \exp\left(\frac{3532.2}{T}\right) P_{\mathrm{HNO_3}}^{1/2.3} \frac{\rho_{ice}\, N_A}{M_{\mathrm{H_2O}}}$$

~~where T is the snow temperature (), $P_{\mathrm{HNO_3}}$ is the partial pressure of (Pa) and $M_{\mathrm{H_2O}}$ is the molar mass of . Note that the co-condensation was excluded in these model runs for a direct comparison between the two different approaches. Both the 'Equilibrium' and 'Kinetic' approaches~~ . Both the configurations resulted in a very similar trend and variation until mid Sept. Despite the '~~Kinetic~~Model 1 - BCice' approach yielding a larger ~~C_v(RMSE)~~ $C_v(\mathrm{RMSE}) = 0.65$ compared to the ~~'Equilibrium' approach~~ "Bock-BC1' approach $C_v(\mathrm{RMSE}) = 0.52$, (~~$C_v$(RMSE) = 0.65 & 0.52, respectively,~~ Table. 2), the '~~Kinetic~~Model 1 - BCice' approach captures the temporal pattern from mid September till early November ~~, yet, the 'Equilibrium' approachdoes not~~but not in the 'Bock-BC1' approach.

5.1.2 Summer

The average temperature ($\pm 1\sigma$) from late spring to early autumn is 240.0 ($\pm$5.0) K (Fig. 3a) and the dominant process determining the snow nitrate concentration are solvation ~~in DI coupled to~~ into the DI coupled with solid state diffusion in Model 1 and partitioning of nitrate to the liquid micropockets in Model 2.

Model 1 captures some trends observed in early spring and during the summer period, including the decrease in concentration of nitrate from the beginning of February, the rise between mid and late November, and the sharp increase in mid December (Fig. 5a). It also reproduced the steep decrease

in concentration at the beginning of 2010 (Fig. 5a) . However, Model 1 (with ~~T_0~~ T_o = 238 K) did not capture the peak in early February and overestimated the concentration of nitrate by a factor of 1.5-5 in December (Fig. 5 ~~a~~A).

The results from Model 2 agreed reasonably well with the observation in these few months with $C_v(RMSE)$ of 0.67. With the contribution from the partitioning of HNO_3 in the micropockets, the features in early February and the peaks between November and mid December were captured (Fig. 5 ~~b~~B). The model underestimates the the nitrate concentration from mid December until January 2010 by a factor of 3. During the summer period, the partitioning into the micropockets contributed $\sim$75% ~~of~~ to the total NO_3^- concentration.

5.2 Halley

Model results for Model 1 and Model 2 in Halley (Fig. 7 and Table. 3) are presented by the season - Late Autumn to Winter (April - Mid September) and Spring to Early Autumn (Mid September - February).

5.2.1 Late Autumn to Winter

The mean temperature ($\pm 1\sigma$) during this period at Halley is 244.72($\pm$7.7) K (Fig. 4a). During this period, the temperature was mostly above the threshold temperature (~~T_0~~ T_o = 238 K, purple shaded area in Fig. 7 A) used in Model 1 but below the eutectic temperature for a H_2O-NaCl mixture (~~251~~ 252 K, yellow shaded area in Fig. 7 B) used in at Halley in Model 2. Therefore, the main process controlling the concentration of NO_3^- in Model 1 is solvation into the DI whereas in Model 2 the main controlling processes are the combination of non-equilibrium adsorption and co-condensation coupled with solid-state diffusion. Performance of Model 1 was poor ($C_v(RMSE)$ = 27.78), overestimating the concentration of NO_3^- by two orders of magnitude (Fig. 7 ~~a~~A). However, some of the trends were reproduced during this cold period such as the two small peaks in mid April and early May, and the rise in mid September (Fig. 7 ~~a~~A).

The modelled results from Model 2 ($C_v(RMSE)$ = 1.08) were a much closer match to the observations compared to Model 1. It captured the first peak in mid April and the small peak in beginning of September ~~.~~(Fig. 7 B). However, it did not reproduce the peak in mid August and underestimated the NO_3^- concentration for the majority of the time.

The results from 'Bock-BC1' and 'Model 1 - BCice' are shown in Fig. 6b. Similar to the Dome C site, the ~~'Equilibrium' approach after Bock et al. (2016) was run alongside the 'Kinetic' approach from late autumn until winter, again, no co-condensation processes were included in these 2 runs for a direct comparison. The~~ modelled results from both approaches are very similar in value and temporal variations ~~(Fig. 6b). Both the 'Kinetic' and 'Equilibrium' approach~~ and both the configurations failed to reproduce the peak in mid August.

5.2.2 Spring to Early Autumn

Similar to the winter months, Model 1 overestimated the bulk NO_3^- concentration at Halley by an order of magnitude and failed to capture any of the variability (Fig. 7 ~~a)~~ A) with $C_v(RMSE)$ = 89.28. Model 2, however, reproduced some features during the warmer months, such as the peak in late September followed by a steady rise in October, the spikes in mid December, beginning of and mid January and also the peak and trough in late January (Fig. 7 ~~b~~B). The partitioning to the micropockets contributed ~80% of the total NO_3^- concentration during this period. ~~The model results~~ Results from Model 2 are within the same order of magnitude compared to the observations ($C_v(RMSE)$ = 0.65, Table. 3).

6 Discussion

The results from both Model 1 and 2 show that the bulk NO_3^- concentration in surface snow can be reasonably well described by non-equilibrium adsorption and co-condensation coupled with solid-state diffusion during autumn to spring at Dome C and in winter at Halley, i.e. when it is cold and the solar irradiance is small. In the summer months, the combination of warmer temperatures and a larger range of diurnal temperature causes the 'Air-Ice' only processes to no longer provide an accurate prediction. The concentration of NO_3^- in the surface snow, during the warmer months, is mainly determined by solvation into DI in Model 1 or partitioning into micropockets in Model 2.

Overall, the results from Model 1 match reasonably well with the year-round observations at Dome C ($C_v(RMSE)$ = 1.34). However, for Halley, Model 1 overestimated the concentration by two order of magnitude ($C_v(RMSE)$ = 89.28). On the other hand, results from Model 2 agree well for both study sites ~~all~~ year-round ($C_v(RMSE)$ = 0.84 for both Dome C and Halley). The mismatch between the models and observations can be separated into 2 categories - data limitations and model configurations, and will be discussed below.

The temporal resolution of the concentration of atmospheric nitrate at both study sites was roughly 5 to 10 days, therefore, any substantial changes in the atmospheric input within a short time scale might be missed and consequently the relative changes in concentration of nitrate in snow might not be observed. Secondly, the vertical snow pit profile of NO_3^- at Dome C (and sites with a low accumulation rate) tended to have a maximum concentration of NO_3^- at the surface of the snowpack (Röthlisberger et al., 2000), especially during the summer period, and the concentration of NO_3^- decreases sharply with the depth ~~inf~~ in the snowpack. The skin layer is the most responsive layer of snow to the changes in the concentration of HNO_3 in the atmosphere above. The snow samples from Dome C were collected carefully from the top 4 ± 2 mm while the snow samples from Halley were collected from the top 25 mm. It is possible that the snow NO_3^- concentrations measured at Halley may be 'diluted' from deeper snow, with a smaller nitrate concentration than the surface ~~, layer~~layer, leading to a positive model bias.

Thirdly, atmospheric nitrate can be ~~find in a more stable~~ found in the particulate forms of NO_3^-, i.e. associated with Na^+, Ca^{2+} or Mg^{2+} (Beine et al., 2003). An increase in sea salt aerosol concentration can shift gaseous HNO_3 to particle-phase (i.e. $NaNO_3$, Dasgupta et al., 2007), ~~hence~~and therefore, decreases the ratio of gaseous HNO_3 ~~to~~ and the total atmospheric nitrate. At Dome C, the atmospheric sea salt aerosol concentration ~~has a strong seasonal variability. The maximum sea salt aerosol concentration tends to be in the~~ in late winter or early spring ~~which can be~~ can be up to a factor of 4 larger than the annual mean ~~(Legrand et al., 2016)~~($\sim 5\ ng\ m^{-3}$, Legrand et al., 2016) due to the large sea ice extend (Jourdain et al., 2008). Therefore, using the total measured atmospheric nitrate as gaseous HNO_3 for constraining the models might ~~cause the mismatch between the modelled results and observations~~ lead to an overestimate of $[NO_3^-]$ in snow at Dome C, especially ~~around Novemeber.~~ in early summer. At the coastal site of Halley, there is a strong influence from sea salt aerosol with corresponding larger concentration of nitrate containing aerosol, especially in spring time that the monthly mean $p-NO_3^-$ mixing ratio is $\sim 4.6\ pptv$ (Rankin et al., 2003; Jones et al., 2011). Therefore, neglecting the dry deposition of nitrate aerosols might underestimate the concentration of nitrate in the surface snow in spring time. The concentration of $p-NO_3^-$ (data not show here, see Jones et al., 2008 for more information) is typically 2.6 and 3.0 times higher than the concentration of nitric acid in winter and summer, respectively, but was up to 8.3 times higher in spring during 2004-2005 at Halley. This might explain the underestimation of concentration of nitrate in surface snow in winter and spring at Halley.

Lastly, no detailed information is available on timing and amount of snowfall events for the time periods in question at both study sites. Single snowfall events can increase the nitrate concentration in surface snow by up to a factor of 4 above the background (Wolff et al., 2008). The contribution of snow nitrate from fresh precipitation ~~maybe~~ may be less important at low accumulation sites, such as Dome C ~~- 27 (Röthlisberger et al., 2000),~~ compared to sites with large snow accumulation like Halley~~~480 (Arthern et al., 2006)~~. Wolff et al. (2008) reports that the large concentration of NO_3^- recorded from mid until end of August was due to new snowfall, which explains why both models failed to reproduce the peak. In the following sections, various processes included in Model 1 and 2 will be discussed.

6.1 ~~'~~Kinetic 'Model 1-BCice' Approach vs ~~'~~Equilibrium 'Bock-BC1' Approach~~The 'Kinetic~~

The 'Model 1-BCice' approach defines the snow grain boundary concentration of NO_3^- by non-equilibrium, kinetic surface adsorption while the '~~Equilibrium~~Bock-BC1' approach after Bock et al. (2016) defines the concentration of the outermost layer of the snow grain (outermost layer thickness = ~~0.5-1.5~~ 1.5 µm~~in this study~~) by thermodynamic equilibrium ice solubility. Both approaches describe the interaction between air and ice, therefore, only results from the winter period are compared. For both sites, the '~~Kinetic~~Model 1-BCice' and '~~Equilibrium~~Bock-BC1' approach resulted in very similar trends except the peak in late October at Dome C (Fig. 6, Table 2 & 3), of which

the '~~Kinetic~~Model 1-BCice' approach managed to reproduce but not the '~~Equilibrium~~Bock-BC1' approach.

The peak of snow nitrate in late October at Dome C corresponds to an increase in atmospheric HNO_3 (Fig. 3 ~~b~~B). The grain surface concentration of the '~~Equilibrium~~Bock-BC1' approach is a function of the partial pressure of HNO_3 with an exponent of 1/2.3 (Eq. 18), while the concentration of the grain boundary defined by the '~~Kinetic Approach'~~ Model 1- BCice' approach is linearly related to the concentration of atmospheric nitrate (Eq. 8). Therefore, the '~~Kinetic~~Model 1- BCice' approach is more responsive to any changes in the atmospheric nitrate concentration compared to the '~~Equilibrium~~Bock-BC1' approach. Other advantages of the former approach are, 1) dynamic characteristics of the grain surface due to changing temperature gradients are taken into consideration; 2) applicability even for sites with high accumulation rates where the skin layer is buried by subsequent snowfall before reaching equilibrium.

At Halley, in winter, the concentrations of NO_3^- are underestimated by both approaches (Fig. 6 and Table 3). There are 2 possible explanations. First, the SSA values used ~~maybe~~ may be underestimated and lead to an underestimation ~~on~~ of adsorption or dissolution in the outermost layer of the snow grain, further field observations are required to verify this. Secondly, due to higher temperatures at Halley compared to Dome C, other processes might be involved in controlling the snow surface concentration of NO_3^-, such as snowfall (not included in the models) or partitioning into liquid micropockets in Model 2 (discussed in Sect. 6.4).

6.2 Co-Condensation - 'Air-Ice' Interaction

The process of co-condensation/sublimation is considered as part of the 'Air-Ice' interaction in both Models 1 and 2. It is driven by the difference in water vapour density across the skin layer snow and the overlying atmosphere. The water vapour density gradient depends exponentially on the temperature gradient. At Dome C the temperature is extremely low and relatively dry, especially in winter, and therefore it is not surprising that only 2% of the grain surface concentration of NO_3^- is from co-condensation during winter and spring (Fig. 6 ~~a~~A, difference between the light and dark blue line). In contrast, at Halley, where winter is warmer and it is relatively humid, $\sim$21% of the grain surface concentration is contributed by co-condensation during winter (Fig. 6 ~~b~~B, difference between the light and dark blue line). As shown in Table 3, the $C_v(\mathrm{RMSE})$ decreased slightly in winter after including co-condensation as part of the 'Air-Ice' interaction. In the summer, the dominant process in Model 1 is solvation ~~in~~ into the DI (See Sect. 6.3) while in Model 2 the dominant process is partitioning ~~in~~ into the micropockets (See Sect. 6.4), hence the contribution from co-condensation to the skin nitrate concentration is insignificant.

There are a few possible sources of uncertainties in the calculation of co-condensation/sublimation processes. For example, the macro-scale gradients of water vapour pressure (across a few mm) were used instead of micro-scale gradients (across a few µm) and there were no precise mea-

surements of skin layer snow density. Uncertainty in the density would lead to uncertainty in the modelled skin layer snow temperature ~~.~~ (Eq. 12). Despite the potential errors in the calculation of co-condensation, the large NO_3^- concentrations in the skin layer in the summer are unlikely to be driven by co-condensation. An unrealistically large average rate of volume change, $\frac{dV}{dt}$, of 130 and 118 $\mu m^{-3}\,s^{-1}$, equivalent to an average grain volume increases of 170% and 135% per day, would be required for Dome C and Halley respectively if the large concentration of NO_3^- in summer was contributed by co-condensation ~~.~~ (Eq. 9 & 10). Assuming the RH ~~of~~ in the open pore space of the skin layer snow to be 100% and RH of the overlying atmosphere ~~is~~ to be the same as measured at 1 m above snowpack, a macro-temperature gradient as high as 2.7×10^3 K m^{-1} would be ~~require~~ required across the top 4 mm of the snowpack to match the large concentration of bulk NO_3^- in the summer at Dome C and in an average temperature gradient of 500 K m^{-1} would be required across the top 10 mm of the snowpack ~~in Halley, which~~ at Halley. Therefore, the required temperature gradients are 1- 2 orders of magnitude ~~higher than observations (Frey et al., 2013) and the modelled temperature gradient (listed in Sect. 3.1.1).~~ larger than indicated by observations or modelled result (Frey et al., 2013, and as listed in Sect. 3.1.1).

6.3 Disordered Interface - Model 1 (~~Temperature >~~ T > T_o = 238 ~~K~~K)

In Model 1, the interfacial layer between air and snow grain is described as 'Air-DI' ~~when the ambient temperatures are above the threshold temperature, T_0~~ T> T_o = 238 K. Therefore, at Dome C, the 'Air-DI' regime applies only during summer months due to the extremely cold temperatures in winter, whereas, at Halley most of the time the interface is considered as 'Air-DI'. The model simulations suggest that an 'Air-ID' interface above 238 K (the lower end of the DI detection limit of pure ice~~(Domine et al., 2013)~~, see Domine et al. (2013)) leads to an overestimation of nitrate concentration in early December at Dome C and all year round at Halley.

The onset temperature for observation of DI on pure ice varies with different experimental setups, probing techniques and how the samples were prepared (Bartels-Rausch et al., 2014). Conde et al. (2008) also found a small fraction of water molecules beginning to leave the outermost crystalline layer of the ice and becoming mobile at 100 K below the melting point of that particular mixture of H_2O and impurities and the number of mobile molecules increases with increasing temperature. When the temperature is ~~larger~~ higher than 10 K below the melting point, molecules might even begin to leave the deeper crystalline layer. The existence of DI not only depends on temperature, but also the speciation and quantity of impurities present within the snow grain (McNeill et al., 2012). Different impurities have different impacts on the hydrogen bonding network at the ice surface and hence have a different impact on the characteristics, such as thickness, of the DI (Bartels-Rausch et al., 2014). Therefore, the chosen threshold temperature, ~~T_0~~ T_o, might be substantially different from what would be found in natural snow or it might not be representative enough to be used as the threshold all year-round (See Sect. 6.5 for the sensitivity analysis regarding to ~~T_0~~ T_o).

Moreover, the partitioning coefficient ~~and mass transport coefficient~~ of the DI were assumed to be the same as those in the aqueous phase and the diffusivity of the DI to be same as those in ice. These assumptions might not be realistic and could lead to overestimation of solvation of HNO_3 ~~in the DI~~ into the DI or overestimate the diffusion from surface of the grain into the bulk ice. However, the real values for partition and ~~mass transport coefficients~~ diffusivity are difficult to measure with the current measurement techniques and need to be re-examined in the future.

There are ~~2~~ 3 possible explanations for why Model 1 provided a reasonable estimation of skin layer snow NO_3^- concentration at Dome C, but not at Halley. Firstly, the chemical composition of surface snow at Dome C is relatively simple, dominated by nitrate anion, which would induce insignificant changes to the hydrogen bonding network at the DI surface compared to a more complicated snow composition (Bartels-Rausch et al., 2014) suggesting the surface properties of snow at Dome C are likely to be comparable to pure ice. Secondly, the temperature at Halley occasionally rises above 0 °C potentially causing melting and significant changes in snow grain morphology at the surface especially. Thirdly, laboratory experiments had shown physical properties, such as extinction coefficient and refractive index, of the ice surface gradually change from the measured value of ice to the measured value for water and the the layer of disordered water molecules grows increasingly thicker as temperature approaches to the melting point (Huthwelker et al., 2006). As temperature increases the DI may become more distinct from ice and more isolated from the bulk and may have less or even no interaction with the bulk.

6.4 Micro-Liquid Pocket - Model 2 (~~Temperature > Eutectic Temperature~~$T \geq T_e$)

Model 2, which includes non-equilibrium surface adsorption and co-condensation coupled with solid diffusion within the grain and partitioning in liquid micropockets, successfully reproduces the concentration of NO_3^- of the surface snow without any tuning parameters for both Dome C and Halley all year round. This is a crucial outcome as it indicates that Model 2 can be used for predicting the air-snow exchange of nitrate at the surface for a wide range of meteorological and depositional conditions that typical for the entire Antarctica.

The liquid water fraction is a function of the total ionic concentration (Eq. 4). Hence, neglecting the existence of other ions may lead to underestimation of the micropocket volume. The additional liquid would increase the dissolution capacity of HNO_3 and hence increase the estimated NO_3^- concentration. As shown in Fig. 7 ~~b~~B, the estimated bulk NO_3^- concentration followed a similar trend as the 'other ions concentration'~~(~~, which is the observed Cl^- concentration~~)~~. Despite NO_3^- being the major anion in the surface snow in Dome C, other anions, such as Cl^- and SO_4^{2-}, were also detected from the same samples (Udisti et al., 2004). Jones et al. (2008) also measured SO_4^{2-} along with Cl^- and NO_3^- from the surface snow samples from Halley. The mismatch between modelled and observed nitrate concentration in the summer can be explained by assuming nitrate to be the only impurity at Dome C, or nitrate and sea salt as the only impurities at Halley. Nevertheless, the

underestimation of the NO_3^- concentration due to underestimating the liquid-water content may be compensated or even overwhelmed if atmospheric deposition of other acids such as HCl or H_2SO_4 increases, which lowers the pH and reduces the solubility of HNO_3 in the micropocket.

Note that the micropockets only exist above the eutectic temperature. For simplification, the eutectic temperature was based on a system containing H_2O and the most abundant solute within surface snow. However, in reality, the presence of other impurities might have an impact on the eutectic temperature. Moreover, the liquid in the micropocket is assumed to behave ideally and, therefore, Henry's coefficient is used to describe the partitioning between air and the micropocket. In reality, there may be some deviation from ideality as the concentration of solutes in the micropocket is likely to be too large to be considered as an ideal dilute solution. The non-ideality should be accounted for in terms of activity coefficient, γ. At equilibrium, the relationship between a solute B and the solvent can be expressed as follow (Sander, 1999):

$$K_B = \frac{\gamma_B x_B}{P_B} \tag{20}$$

where P_B is the vapour pressure of B, γ_B is the activity coefficient of B and x_B is the mole fraction of B. The value of the activity coefficient approaches unity as the mole fraction of B approaches zero ($\gamma_B \to 1$ as $x_B \to 0$) and, under such ideal-dilute condition, the equilibrium constant, K_B, is defined as Henry's law coefficient. Values of activity coefficient can be found experimentally. The available parameterisation of activity coefficient of HNO_3(aq), H^+ and NO_3^- is only accurate for concentration up to 28 m (Jacobson , 2005). When the molarity is higher than ~4-5 m, depending on the temperature, the activity coefficient of H^+ and NO_3^- increases as molarity increase. The concentration of the micropocket is estimated based on the parameterisation by Cho et al. (2002), which predicts a concentration a lot larger than the limit of activity coefficient parameterisation available at present. Hence, it is not possible to quantify the uncertainties caused by assuming the micropocket has ideal-solution behaviour. If the relationship between activity coefficient and molarity extend to molarity larger than 28 m, the activity coefficient will be larger than 1 and hence reduces the value of the equilibrium constant, K_B, compared to the Henry's Law coefficient. By means, the assumption of ideal-solution behaviour of micropocket is likely to overestimate the concentration of the micropocket. The activity coefficient of highly concentrated solution is needed to be found by further experimental studies.

6.5 Sensitivity Analysis

In order to assess the robustness of the findings presented here they were analysed as a function of model sensitivities to constraints, parameterisations and measurement uncertainties. Parameters were varied one at a time by the given range while keeping all others constraints and parameterisation the same (Table. 4, ~~Col.~~ Column 1~~,~~). The coefficient of variation, $C_v(\mathrm{RMSE})$, was calculated from

each sensitivity test (Table. 4) and compared with the $C_v(RMSE)$ of the 'Control', which uses the observed values and parameterisation listed in Sect. 4 and Table. A1.

Both Model 1 and 2 are sensitive to the concentration of HNO_3 in the air and the concentration of NO_3^- in snow. Reducing concentration of HNO_3 in the atmosphere by 20% or increasing the concentration of NO_3^- in snow by 20% improves the performance of both models. This supports the suggestion that the atmospheric nitrate observed at Dome C only represents the upper limit of nitric acid and it is likely to lead to an overestimation of the concentration of nitrate in snow (Sect. 6) while at Halley, the skin layer snow might well be 'diluted' by snow sample from the deeper layer (Sect. 6).

Both models are sensitive to the value of SSA as a smaller SSA implies a smaller surface area per unit ~~volumn~~ volume of snow, and hence, less surface sites available for adsorption per unit ~~volumn~~ volume of snow. It has a more notable impact in Model 1 and in the winter, when the grain boundary processes play an important role for the overall snow nitrate concentration due to the cold temperature. A similar explanation applies the value of the maximum number of adsorption site, N_{max}. However, varying the accommodation coefficient, α, by $\pm$ 10% does not have a significant impact on the performance of the models (Table 4).

Model 1 is very ~~sensitivity~~ sensitive to the threshold temperature, ~~T_0~~T_ϱ. At Dome C, the best match (lowest $C_v(RMSE)$) between modelled and observation is with a threshold temperature 2 K larger than the control ~~T_0~~ T_ϱ = 238 K. However, increasing ~~T_0~~ T_ϱ to 242 K worsens the model performance further (Fig. 5A, Green line & Table 4). In general, the grain boundary concentration of nitrate defined by solvation into the DI is much larger than when it is defined by the combination of surface adsorption and co-condensation on ice. A larger temperature is required to assume the interface is 'Air-DI' when a large value of ~~T_0~~ T_ϱ is used. At Dome C, a larger value of ~~T_0~~ T_ϱ may have reduced the overestimation in late November due to a larger fraction of time falling below the threshold but compromised the good fit from mid December onward and yield a higher $C_v(RMSE)$. At Halley, despite the improvement in $C_v(RMSE)$ when a higher temperature threshold was used, the modelled $[NO_3^-]$ is still an order of magnitude larger than the observation (Fig. 7 ~~b~~B).

Model 1 is not sensitive to the pH of the DI layer. Even though the effective Henry's law coefficient increases by an order of magnitude when pH increases from 5 to 6.5 (Fig. A3), the $C_v(RMSE)$ remains the same. This behaviour can be explained by the combination of the kinetic approach and slow diffusion rate of nitrate in ice that the rate of change in the grain boundary concentration remains small even the boundary concentration increases.

Model 2 is sensitive to the eutectic temperature, T_e, but not as much as for ~~T_0~~ T_ϱ in Model 1. Increasing T_e in Model 2, only improves the performance at Dome C but not Halley. Higher T_e implies that a larger temperature is required for the co-existence of liquid micropockets. For Dome C, increasing T_e by 2-4 K reduces the overestimation in November without compromising

the results from mid December onwards, as the average temperature during that period was higher than $T_e = 234$K.

7 Conclusions

Two surface physical models were developed from ~~first principles~~ physical parameterisations and laboratory data to estimate the bulk concentration of NO_3^- in the skin layer of snow ~~using~~ constrained by observed atmospheric nitrate ~~concentration~~concentrations, temperature and humidity~~as inputs.~~.

Model 1 ~~is based on the assumption of a homogeneous~~ assumes that below a threshold temperature, T_o, the outermost layer of a snow grain is pure ice, whereas above T_o the outermost layer is a disordered interface (DI)~~as the interface between air and snow grain above 238 and Model 2 is based on the hypothesis of the majority of the snow crystal surfaces being ice, and above the eutectic temperature a liquid exists in grooves at grain boundaries and triple junction.~~

. The nitrate concentration at the air-ice boundary is defined by non-equilibrium kinetic adsorption and co-condensation whereas the nitrate concentration at the air-DI boundary is defined by non-equilibrium kinetics based on Henry's Law. An non-equilibrium grain boundary is assumed as the partial pressure of HNO_3 is low in Antarctica and a large temperature gradient is expected across the snowpack surface which leads to redistribution of water molecule at the grain surface. The boundary of the grain is also assumed to be interacting with the bulk that the mass transport is driven by the concentration difference between the boundary and centre of the grain and constrained by solid-state diffusion. The uncertainties of Model 1 are 1) the temperature threshold, T_o, that defines the onset of 'air-DI' interface; 2) the partitioning coefficient of HNO_3 into the DI; and 3) the interaction between the grain boundary and the bulk ice. The modelled skin layer concentration of NO_3^- from Model 1 agreed reasonably well with observations at Dome C but overestimated observations by an order of magnitude at the relatively warmer Halley site. The ~~uncertainties in Model 1 are the temperature threshold, T_o, that defines the onset of 'Air-DI' interface and the partition coefficient of DI. The~~ poor performance of Model 1 at the ~~warmer site supports the argument in previous studies (Bartels-Rausch et al., 2014; Domine et al., 2013) that the disordered interface cannot be parameterised as a thin, homogenous water-like layer covering the entire grain surface or that its air-DI partitioning is the same as air-liquid partitioning.~~ warmer site suggests that as the temperature increases the disordered interface is becoming more liquid-like and disconnected from the bulk ice.

Model 2 assumes that below melting temperature, T_m, the outermost layer of a snow grain is pure ice and above eutectic temperature, T_e, liquid exists in grooves at grain boundaries and triple junctions as micropocket. The nitrate concentration at the air-ice boundary is defined by non-equilibrium kinetic adsorption and co-condensation. The boundary of the grain is also assumed to be interacting with the bulk and the mass transport between the surface and centre of the grain is driven by solid-state diffusion. The nitrate concentration of the liquid micropocket is defined by Henry's law.

Equilibrium between air and liquid in micropockets is assumed because the liquid micropocket volume is small and HNO_3 is very soluble in water implying fast interfacial mass transport. The main uncertainties in Model 2 are three-fold, 1) dry and wet deposition of atmospheric nitrate are currently not included in the model, but lead to episodic increases of NO3 in surface snow; 2) the liquid micropocket is likely not an ideal solution due to high ionic strength; and 3) third the eutectic temperature of natural snow is assumed to be that of a single major ion - water system but may be different because snow ionic composition is complex. However, Model 2 reproduced the skin layer concentration of NO_3^- with good agreement at both Dome C and Halley without any tuning parameters. ~~Thus the major interface between skin layer snow grain and surrounding air can well be described as 'Air-Ice' with a liquid formed by impurities present as micropockets as suggested by Domine et al. (2013). In~~

Both Model 1 and 2 suggest that in the winter the interaction of nitrate between the air and skin layer snow can be described as a combination of non-equilibrium kinetic ice surface adsorption and co-condensation coupled with solid diffusion within the grain. ~~In~~ Only Model 2 provides a reasonable estimate at both sites year-round, that suggests in the summer, the major interface between snow grain and surrounding air is still air-ice, but it is the equilibrium solvation into liquid micropockets that dominates the exchange of nitrate between air and ~~skin layer snow.~~ snow. Despite the simplified parameterisation of processes in Model 2, it provided a new parameterisation to describe the interaction of nitrate between air and snow as 'air-ice' with a liquid formed by impurities present as micropockets as suggested by Domine et al. (2013) instead of an 'air-DI' interface assumed by most models developed previously. Moreover, the non-equilibrium boundary between air and snow grain allows the models to work at sites with high rate of accumulation that the snow layer might be buried by fresh snowfall before reaching equilibrium.

Additional modelling studies, e.g. including uptake of other chemical species ~~or aerosols~~ and aerosols such as H_2SO_4 and nitrate aerosols, backed up by field observations from other locations with various meteorological conditions as well as laboratory studies on the eutectic point of a ~~multi-ions~~ multi-ion - H_2O system, uptake coefficient at a higher temperature, are needed to ~~confirm the representativeness and~~ improve the performance of Model 2.

~~Despite the simplified parameterisation of processes in Model 2, such as the impurities content in snow and the behaviour of the liquid micropockets, it is a excellent step towards parameterising the interactions between air and snow. The~~ Moreover, the models presented here are describing the exchange between air and the skin layer of snowpack as the uptake processes are much quicker than the photochemical loss, and therefore, can be modelled by 'physical-only' processes.

Atmospheric nitrate can reach deeper than the skin layer via wind pumping and temperature gradient, however, the nitric acid concentration in snow interstitial air (SIA) is expected to be small compared to the overlying atmosphere due to the high uptake of nitrate near the surface of the snowpack. A smaller concentration of HNO_3 in SIA implies a smaller uptake in deeper snow, and hence

the photochemical loss cannot be assumed to be negligible in deeper snow. Therefore, a more complex multi-layer model including both physical and chemical processes is required to reproduce the nitrate concentration in deeper snow and ~~being~~ to implement in regional and global atmospheric chemistry ~~model~~models.

Acknowledgements. HGC is funded by the Natural Environment Research Council through Doctoral Studentship NE/L501633/1. We are thankful to our colleagues (Anna Jones, Neil Brough and Xin Yang) for helpful discussion.

8 Notation

Symbol	Description	units
α	Accommodation coefficient	dimensionless
$\mathrm{A_{ice}}$	Surface area of ice per unit volume of snowpack	$\mathrm{m^2\ m^{-3}_{snowpack}}$
$\mathrm{C_v(RMSE)}$	Coefficient of variation	N/A
DI	Disordered Interface	N/A
D_v	Water vapour diffusivity	$\mathrm{m^2\ s^{-1}}$
D'_s	Gas-phase diffusivity in snow	$\mathrm{m^2\ s^{-1}}$
ΔH^0_f	enthalpy of fusion	$\mathrm{J\ mol^{-1}}$
$[\mathrm{HNO_{3\,(ads)}}]$	Nitric acid concentration contributed by surface adsorption	$\mathrm{molecule\ m^{-3}}$
$[\mathrm{HNO_{3\,(cc)}}]$	Nitric acid concentration contributed by co-condensation	$\mathrm{molecule\ m^{-3}}$
$[\mathrm{HNO_{3\,(DI)}}]$	Nitric acid concentration in the DI	$\mathrm{molecule\ m^{-3}}$
$[\mathrm{HNO_{3\,(g)}}]$	Nitric acid concentration in gas-phase	$\mathrm{molecule\ m^{-3}}$
$[\mathrm{HNO_{3\,(ice)}}]$	Nitric acid concentration in solid ice	$\mathrm{molecule\ m^{-3}}$
$[\mathrm{HNO_{3\,(surf)}}]$	Nitric acid concentration on surface of grain	$\mathrm{molecule\ m^{-3}}$
$[\mathrm{Ion_{tot,bulk}}]$	Total ionic concentration in melted snow sample	$\mathrm{molecule\ m^{-3}}$
k_{ads}	Adsorption coefficient on ice	$\mathrm{m^3\ molecule^{-1}\ s^{-1}}$
k_{des}	Desorption coefficient on ice	$\mathrm{s^{-1}}$
$k_{\mathrm{H^{cc}}}$	Henry's Law coefficient	dimensionless
$k^{\mathrm{eff}}_{\mathrm{H}}$	Effective Henry's Law coefficient	dimensionless
k_{diff}	~~Diffusion coefficient~~ Diffusivity in ice	$\mathrm{m^2\ s^{-1}}$
k_w	Thermal conductivity of snowpack	$\mathrm{Wm^{-1}K^{-1}}$
$\mathrm{K_a}$	Acid dissociation constant	$\mathrm{molecule\ m^{-3}}$
$\mathrm{K_{eq}}$	Equilibrium constant for Langmuir adsorption	$\mathrm{m^3\ molecule^{-1}}$
$m_{\bar{\mathrm{H_2O}}}$	Molecular mass of water	$\mathrm{kg\ mol^{-1}}$
N_{max}	Maximum number of adsorption sites	$\mathrm{molecule\ m^{-2}}$
$[\mathrm{NO^-_{3\,(bulk)}}]$	Bulk nitrate concentration	$\mathrm{molecule\ m^{-3}}$
$\phi_{\mathrm{H_2O}}$	Liquid water fraction	dimensionless
$\Phi^{\mathrm{aq}}_{\mathrm{bulk}}$	Fraction of the total amount of solute in aqueous phase	dimensionless
R_{eff}	Effective radius of snow grain derived from SSA data	m
R	Ideal gas constant	$\mathrm{J\ mol^{-1}\ K^{-1}}$
ρ_{ice}	Density of ice	$\mathrm{kg\ m^{-3}}$
ρ_v	Water vapour density	$\mathrm{kg\ m^{-3}}$
[S]	Number of available surface sites per unit volume of air	$\mathrm{molecule\ m^{-3}_{air}}$
SSA	Specific surface area	$\mathrm{m^2\ kg^{-1}}$
T_e	Eutectic temperature	K
T_f	Reference temperature	K
T_o	Threshold temperature in Model 1	K
θ	Fraction of surface sites being occupied	dimensionless
$\overline{v}$	Mean molecular speed	$\mathrm{m\ s^{-1}}$
V_{air}	Volume of air per unit volume of snowpack	$\mathrm{m^3_{air}\ m^{-3}_{snowpack}}$
V_{grain}	Volume of a snow grain	$\mathrm{m^3}$

Table 1. Characteristic times associated with gas-phase diffusion, mass transport and uptake of gas into ice grain

Process	Expression	Order of magnitude, s
Interfacial mass transport to a liquid surface[i]	$\frac{3\overline{v}\alpha_{aq}}{4R_{\rm eff}}$ ~~$\frac{4R_{\rm eff}}{3\overline{v}\alpha_{aq}}$~~	10^{-7}
Gas-phase diffusion to the surface of a spherical droplet[ii]	$\frac{3\,D'_s}{R^2_{\rm eff}}$ ~~$\frac{R^2_{\rm eff}}{3\,D'_s}$~~	10^{-4}
Molecular diffusion between snowpack and the atmosphere[iii]	$\frac{z^2}{D'_s}$	10^{0}
Liquid-phase diffusion within a water droplet[iv]	$\frac{4\,R^2_{\rm eff}}{\pi^2\,k_{\rm diff(aq)}}$	10^{0}
Surface adsorption on ice[v]	$\frac{1}{k_{\rm des}}$	10^{3}
Solid-state diffusion within a snow grain[vi]	$\frac{4\,R^2_{\rm eff}}{\pi^2\,k_{\rm diff}}$	10^{6}
Photolysis at a snowpack surface[vii]	$\frac{1}{J}$	$> 10^{7}$

[i] Sander (1999), with an effective radius, $R_{\rm eff}$ = 70 µm, and accommodation coefficient on liquid water, $\alpha_{aq} = 7.5\times10^{-5}\exp(2100/\mathrm{Temp})$ (Ammann et al., 2013). [ii] Sander (1999), with an effective molecular diffusivity, $D'_s = D_a/\tau_g$, where the tortuosity, $\tau_g = 2$ and molecular diffusivity in free air at 296 K, $D_a(296\mathrm{K}) = 87\ \mathrm{Torr\,cm^2\,s^{-1}}$ (Tang et al., 2014). [iii] Waddington et al. (1996), with a snow layer thickness, z = 4 mm. [iv] Finlayson-Pitts and Jr. (2000), with a diffusion coefficient in liquid water, $k_{\rm diff(aq)} = 1\times10^{-9}\ \mathrm{m^2\,s^{-1}}$ (Yuan-Hui and Gregory, 1974) . [v] Crowley et al. (2010), with an equilibrium constant for Langmuir adsorption, $K_{eq} = 2\times10^{-16}\ \mathrm{m^3\,molecule^{-1}}$ and adsorption coefficient, $k_{\rm ads} = 1.7\times10^{-19}\ \mathrm{m^3\,molecule^{-1}\,s^{-1}}$. [vi] Finlayson-Pitts and Jr. (2000), with a diffusion coefficient in ice, $k_{\rm diff} = 6\times10^{-16}\ \mathrm{m^2\,s^{-1}}$ (Thibert et al., 1998). [vii] Finlayson-Pitts and Jr. (2000), with a surface NO_3^- photolysis rate coefficient, J, = $10^7\ \mathrm{s^{-1}}$ (Thomas et al., 2011).

Table 2. Summary of model performance at Dome C based on the coefficient of variation of RMSE, $\mathrm{C_v(RMSE)}$

Model description	Short name	Whole year DOY 30 - 385	Winter-Spring DOY 90 - 318	Summer DOY 319 - 385
Surface Adsorption & Solid Diffusion	~~Kinetic Approach~~ Model1-BCice	-	0.65	-
Ice Solubility & Solid Diffusion	~~Equilibrium Approach~~ Bock-BC1	-	0.52	-
Surface Adsorption-Co Condensation/DI Solvation & Solid Diffusion				
No threshold (no Solvation)	Model 1-none	1.07	0.65	0.88
~~Threshold $\leq$~~ T_s = 238 K	Model 1-238K	1.34	0.73	1.11
Surface Adsorption-Co Condensation & Solid Diffusion + micropocket	Model 2	0.84	0.73	0.67

Table 3. Summary of model performance at Halley based on the coefficient of variation of RMSE, $C_v(\mathrm{RMSE})$

Model description	Short name	Whole year DOY 87 - 406	Winter DOY 90 - 257	Spring -Early Au DOY 258 - 4
Surface Adsorption & Solid Diffusion	~~Kinetic Approach~~ Model1-BCice	-	1.13	-
Ice Solubility & Solid Diffusion	~~Equilibrium Approach~~ Bock-BC1	-	1.12	-
Surface Adsorption-Co Condensation/DI Solvation & Solid Diffusion				
No threshold (no Solvation)	Model 1-none	1.06	1.06	0.95
~~Threshold $\leq$~~ $T_o =$ 238 K	Model 1-238K	89.28	27.78	87.15
Surface Adsorption-Co Condensation & Solid Diffusion + micropocket	Model 2	0.84	1.08	0.65

Table 4. Sensitivity test for Model 1 and 2 based on the coefficient of variation of RMSE, $\mathrm{C_v(RMSE)}$, the metric was used to measure a goodness of fit. Note that column one is not fitted to the observation and the values are only varying to show the sensitivity of the models against inputs and parameterisation.

Parameter		Model 1						Model 2					
		Dome C			Halley			Dome C			Halley		
		Whole year	Winter-Spring	Summer	Whole year	Winter	Spring-Summer	Whole year	Winter-Spring	Summer	Whole year	Winter	Spring-Summer
Control		1.34	0.73	1.11	89.28	27.78	87.15	0.84	0.73	0.67	0.84	1.08	0.65
$[HNO_3]$	-20%	0.98	0.60	0.81	71.19	22.12	69.5	0.80	0.62	0.64	0.77	1.10	0.56
	$+20\%$	1.73	0.90	1.45	107.36	33.43	104.80	0.95	0.88	0.76	0.92	1.07	0.75
SSA	-10%	1.06	0.63	0.88	79.35	24.79	77.46	0.83	0.67	0.67	0.84	1.10	0.65
	$+10\%$	1.63	0.84	1.36	99.22	30.75	96.86	0.84	0.78	0.67	0.83	1.07	0.65
α	-10%	1.34	0.73	1.11	79.35	24.78	77.46	0.83	0.73	0.67	0.83	1.08	0.65
	$+10\%$	1.34	0.73	1.11	79.35	24.80	77.46	0.83	0.73	0.67	0.83	1.08	0.65
N_{max}	-10%	1.32	0.67	1.10	89.27	27.77	87.15	0.83	0.69	0.67	0.84	1.09	0.65
	$+10\%$	1.36	0.80	1.13	89.29	27.78	87.15	0.84	0.77	0.67	0.84	1.07	0.65
T_o (Model 1) or	-2 K	3.53	0.91	3.00	90.45	42.54	87.31	0.95	0.92	0.75	0.85	1.12	0.65
T_e (Model 2)	+2 K	0.50	0.64	0.36	67.49	25.33	65.62	0.73	0.65	0.58	0.86	1.07	0.65
	+4 K	0.61	0.65	0.47	50.76	23.86	49.00	0.72	0.65	0.57	0.88	1.06	0.67
pH	-0.4	1.34	0.73	1.11	89.28	27.78	87.15	-	-	-	-	-	-
	+0.4	1.34	0.73	1.11	89.28	27.78	87.15	-	-	-	-	-	-
	+0.8	1.34	0.73	1.11	89.28	27.78	87.15	-	-	-	-	-	-
$[NO_3{}^-]$	-20%	1.85	0.98	1.54	111.87	34.84	109.2	0.99	0.96	0.79	1.09	1.08	0.93
	$+20\%$	1.04	0.61	0.86	74.22	23.07	72.45	0.80	0.64	0.64	0.74	1.10	0.51

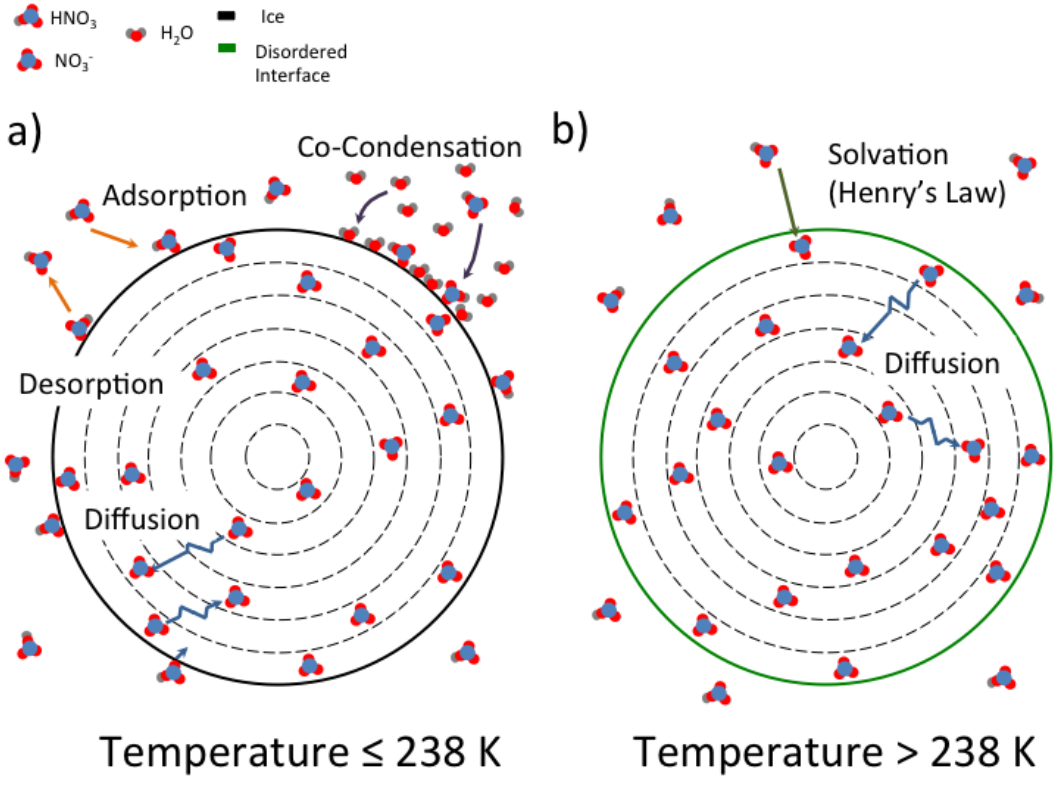

Figure 1. Schematic of Model 1. a) At ~~temperatures below~~ T ≤ 238 K the concentration of NO_3^- at the ~~surface~~ boundary of the snow grain is determined by Air-Ice processes, i.e. non-equilibrium adsorption and co-condensation. b) At ~~temperatures above~~ T > 238 K the concentration of NO_3^- at the ~~surface~~ boundary of the snow grain is determined by Air-DI processes, i.e. non-equilibrium solvation into DI.

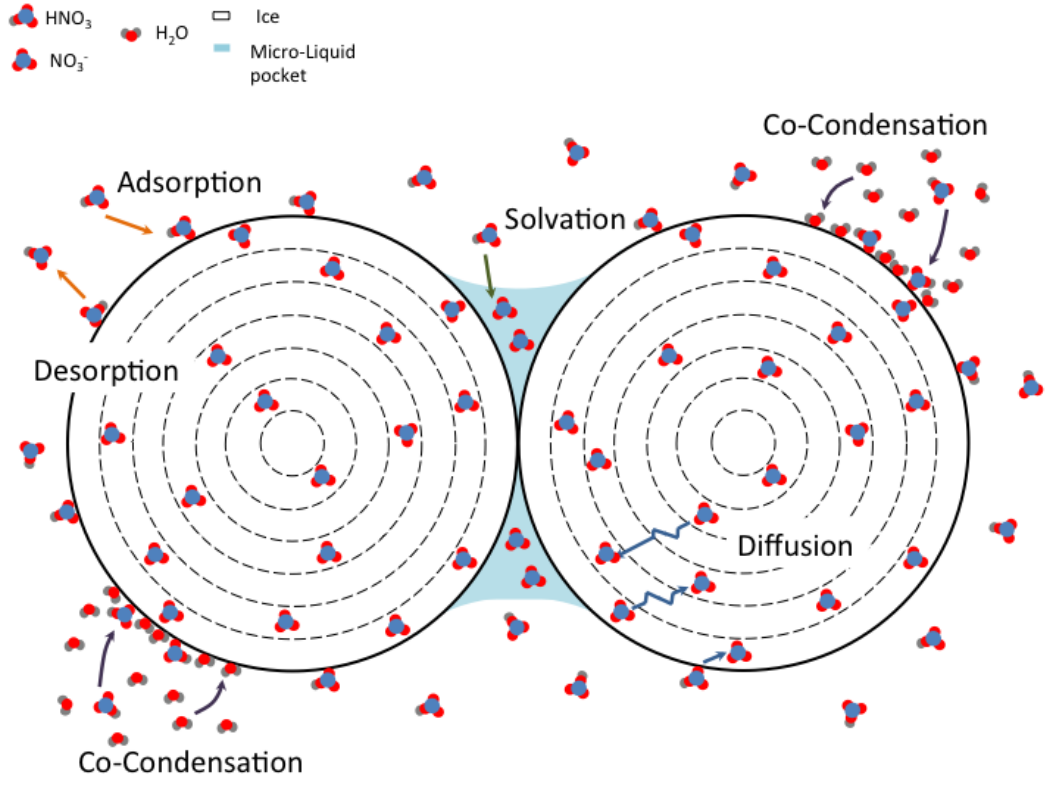

Figure 2. Schematic of Model 2. At ~~all temperatures below melting~~$T < T_m$, the concentration of NO_3^- at the ~~surface~~ boundary of the snow grain is determined by Air-Ice processes, i.e. non-equilibrium adsorption and co-condensation. At ~~temperatures above the eutectic temperature~~$T \geq T_e$, liquid is assumed to co-exist with ice and the liquid fraction is in the form of micropockets that are located at grain boundaries and triple junctions (Domine et al., 2013).

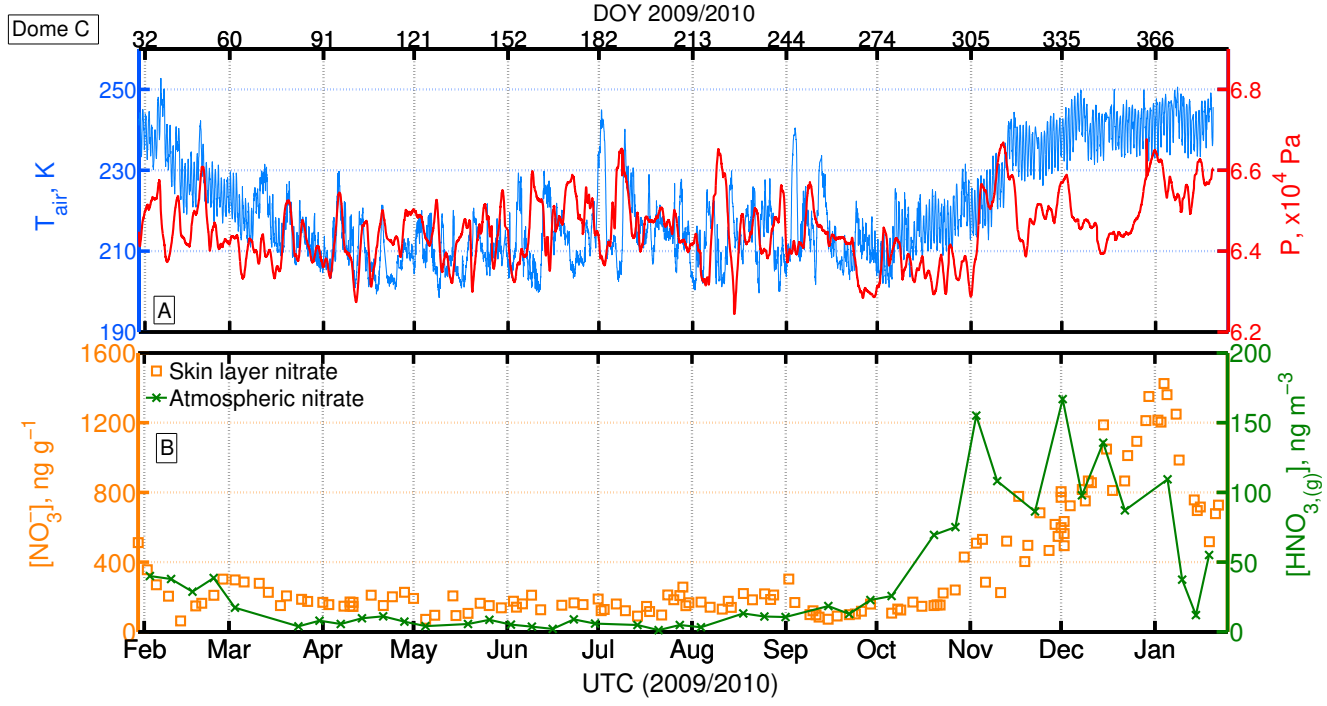

Figure 3. Atmospheric and snow observations from Dome C ~~(published previously by Erbland et al., 2013, Fig. 6~~from Erbland et al. (2013)). (**A**) Air temperature (blue, left axis) and atmospheric pressure (red, right axis). (**B**) NO_3^- in the snow skin layer ~~snow~~ (i.e. top 4 $\pm$ 2 mm~~) nitrate concentrations (~~, orange square, left axis) and atmospheric ~~nitrate concentrations~~NO_3^-, i.e. sum of the atmospheric particulate ~~nitrate~~ NO_3^- and HNO_3 (green, right axis).

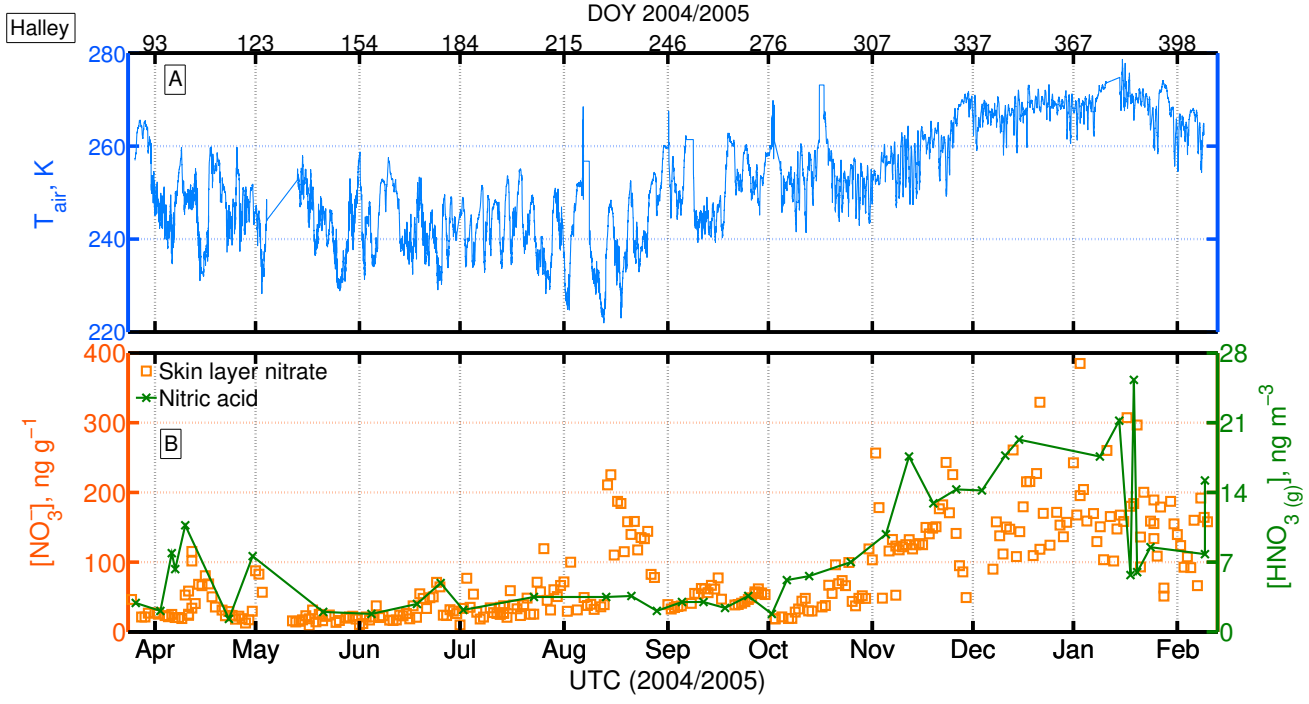

Figure 4. Atmospheric and snow observations at Halley between 27$^{\text{th}}$ March 2004 and 9$^{\text{th}}$ February 2005 ~~(Jones et al., 2008)~~from Jones et al. (2008). (**A**) Air temperature. (**B**) NO_3^- in the surface snow ~~, the~~ (i.e. top 10 ± 15 mm, ~~nitrate concentrations (~~orange square, left axis) and gas-phase ~~nitric acid concentrations~~ HNO_3 (green, right axis).

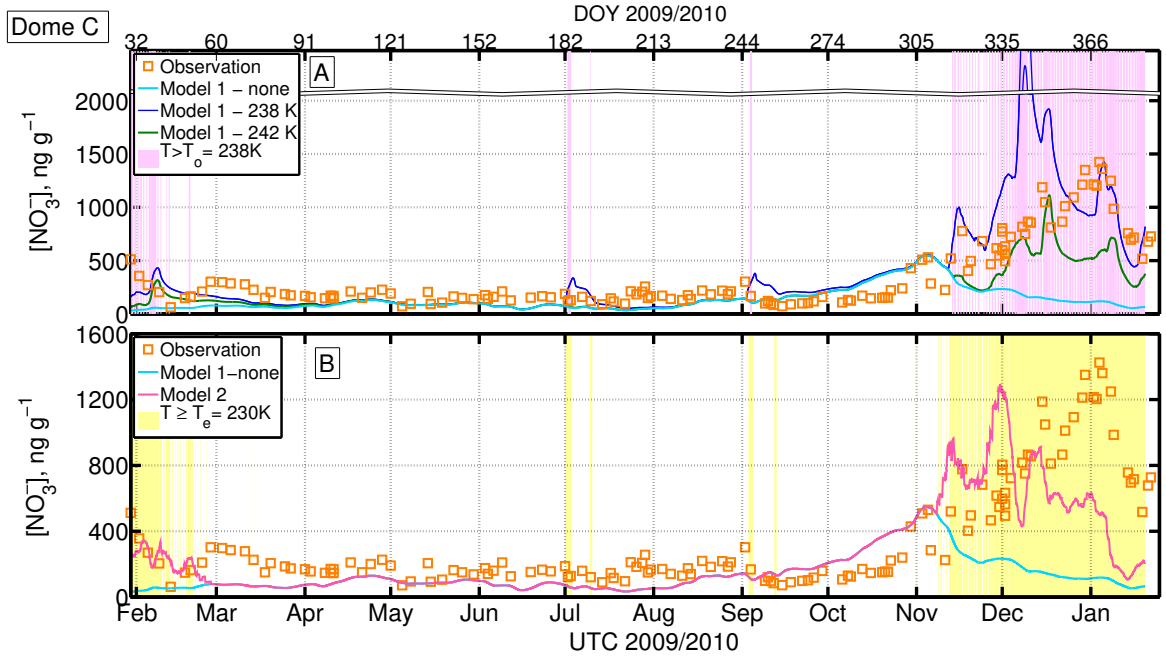

Figure 5. (**A**) Model 1 output of Dome C skin layer snow concentration of NO_3^-. At ~~temperatures less than~~ $T < T_o$ the ~~threshold temperature, T_o, the~~ interface between air and snow grain is assumed to be ice ('Air-Ice') and the NO_3^- concentration is determined by a combination of non-equilibrium adsorption on ice and co-condensation coupled with solid-state diffusion. ~~Above T_o~~At $T > T_o$, the interface between air and snow grain is assumed to be a DI ('Air-DI'), i.e. the NO_3^- concentration is determined by a combination of non-equilibrium solvation ~~in~~ into the DI coupled with solid-state diffusion. Note that the y-axis is broken between 2000-3500 ng g^{-1}. Orange squares: observation~~. Dark~~; Light blue: ~~'Mode~~ Model 1 ~~- 238 '~~with $T_o > T_m$, i.e. only air-ice interaction; Dark blue: Model 1 with T_o ~~set as =~~ 238 K; Green: ~~'Mode 1 - 242 ',~~ Model 1 with T_o ~~set as =~~ 242 K; ~~Light blue: 'Mode 1 - none', Model 1 with T_o set above the melting temperature, i.e. air-ice only interaction~~Purple shaded area indicate times when $T > T_o$ = 238 K; (**B**) Model 2 output of Dome C skin layer snow NO_3^- concentration. The major interface between air and snow is assumed to be ice ('Air-Ice') at ~~all temperatures below melting~~ $T < T_m$ and the NO_3^- concentration in ice is determined by a combination of non-equilibrium adsorption and co-condensation coupled with solid-state diffusion. Above ~~eutectic temperature, T_e~~ ~~($T > T_e$ =~~230 K~~)~~, liquid ~~co-existed~~ co-exists with ice in the form of micropocket. The partition between air and micropocket is determined by Henry's law. Orange squares: observation; Light blue: ~~'Mode 1 - none',~~ Model 1 with ~~T_o set above the melting temperature~~$T_o > T_m$, i.e. air-ice only interaction; Pink: 'Model 2' - air-ice interaction plus micro-liquidpockets; Yellow shaded area indicates times when $T > T_e$ = 230 K (T_e for HNO_3-H_2O system).

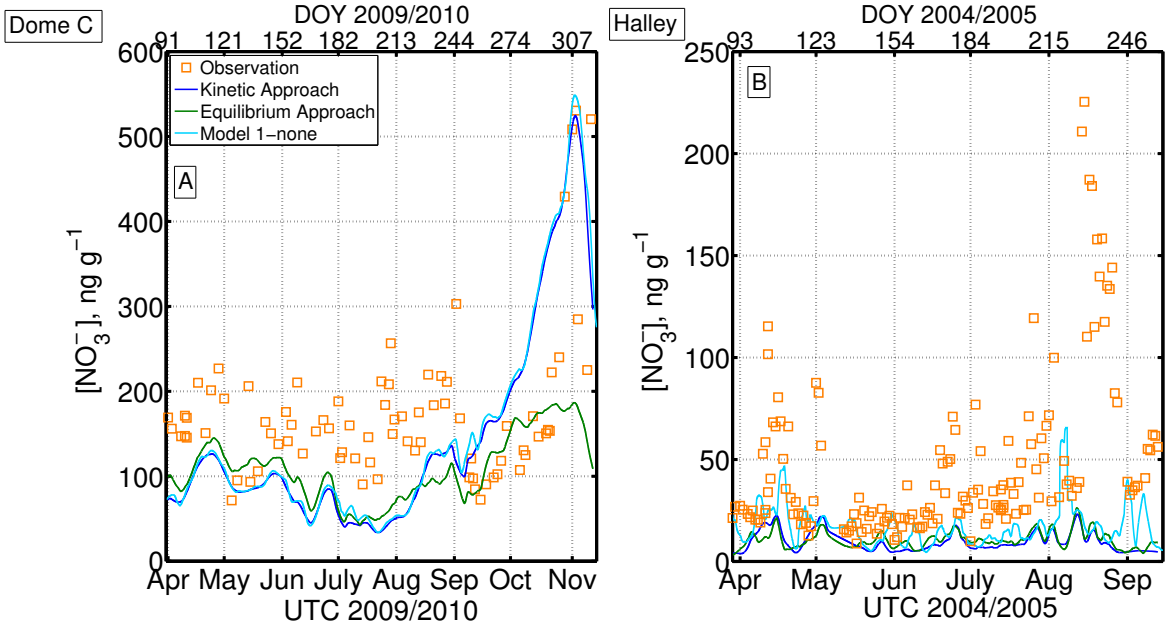

Figure 6. Comparison of the 'Kinetic' approach (this work, in dark blue) with the 'Equilibrium' approach (similar to Bock et al. (2016), in green), and the contribution from the co-condensation process (Results from Model 1- none, in light blue) in winter. The 'Kinetic' approach describes the air-snow interaction of nitrate as non-equilibrium kinetic surface adsorption coupled with solid diffusion inside the grain whereas the 'Equilibrium' approach describes the interaction as equilibrium solubility coupled with solid diffusion inside the grain. The 'Model 1-none' describes the interaction as co-condensation plus non-equilibrium kinetic surface adsorption coupled with solid diffusion within the grain. (**A**) Results at Dome C. (**B**) Results at Halley.

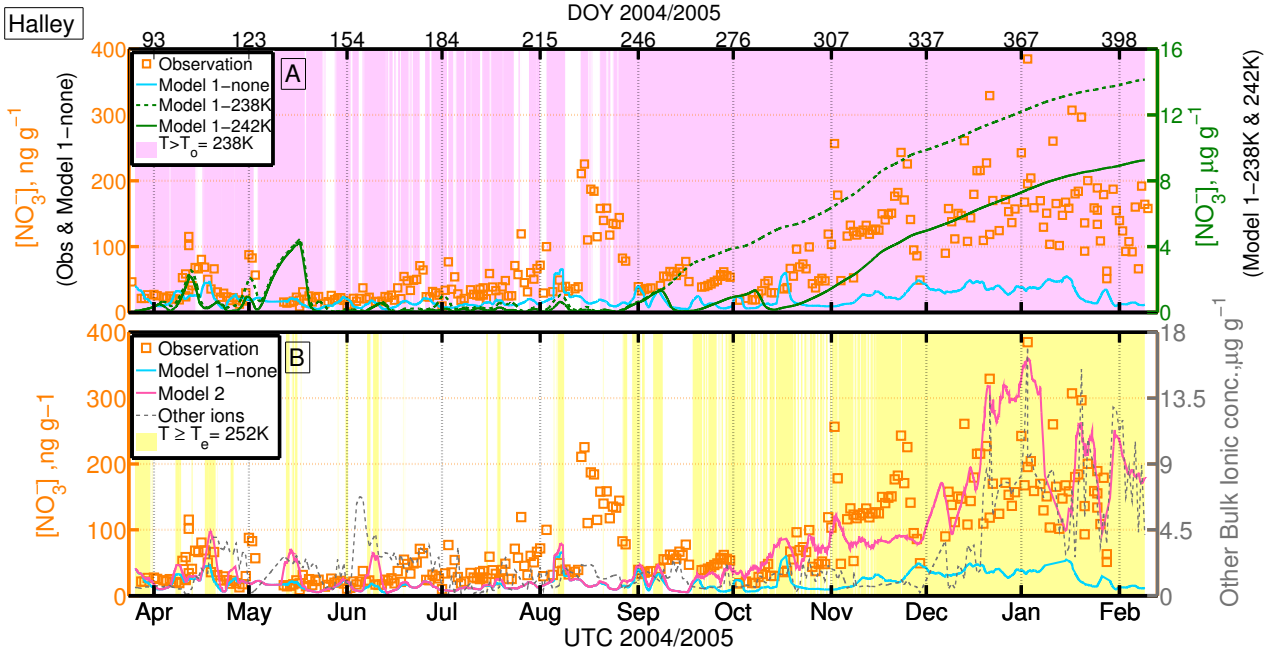

Figure 7. (**A**) Model 1 output of Halley skin layer snow concentration of NO_3^- ~~at Halley~~. At ~~temperatures below~~ $T < T_o$ the ~~threshold temperature, T_o, the~~ interface between air and snow grain is assumed to be ice ('Air-Ice') and the NO_3^- concentration is determined by a combination of non-equilibrium adsorption on ice and co-condensation coupled with solid-state diffusion. At ~~temperature above T_o~~ $T > T_o$, the interface between air and snow grain is assumed to be a DI ('~~Air-Ice~~Air-DI'), ~~where~~ i.e. the NO_3^- concentration is determined by a combination of non-equilibrium solvation ~~in~~ into the DI coupled with solid-state diffusion. Orange ~~square (Left axis) -~~ squares: observation; Light blue~~(Left axis)~~ : ~~'Mode 1 - none',~~ Model 1 with ~~T_o set above the melting temperature~~ $T_o > T_m$, i.e. ~~air-ice~~ only air-ice interaction; ~~Black (Right axis)~~Dark blue: ~~'~~Model ~~1-238 ' - Model~~ 1 with T_o ~~set to~~ = 238 K; ~~Purple (Right axis)~~Green: ~~'~~Model ~~1-242 ' - Model~~ 1 with T_o ~~set to~~ = 242 K~~.~~; Purple shaded area indicate times when $T > T_o$ = 238 K; (**B**) Model 2 output of ~~Halley~~ Dome C skin layer snow NO_3^- concentration. The major interface between air and snow is assumed to be ice ('Air-Ice') at ~~all temperature below melting~~ $T < T_m$ and the NO_3^- concentration in ice is determined by a combination of non-equilibrium adsorption and co-condensation coupled with solid-state diffusion. Above ~~eutectic temperature, T_e (~~$T > T_e$ =252 K~~)~~, liquid ~~co-existes~~ co-exists with ice in the form of micropocket. The partition between air and micropocket is determined by Henry's law. Orange squares: observation; Light ~~Blue~~blue: ~~'Mode 1 - none',~~ Model 1 with ~~T_o set above the melting temperature~~ $T_o > T_m$, i.e. air-ice only interaction; Pink: 'Model 2' - air-ice interaction plus micro-liquidpockets; Grey (Right axis) - measured bulk concentration of other ions, where other ions refers to the sum of $[Na^+]$ and $[Cl^-]$~~.~~; Yellow shaded area indicates times when $T > T_e$ = 252 K (T_e for $NaCl\text{-}H_2O$ system)

Appendix A: Parameterisation

Table A1. Parameterisation for HNO_3

Symbol	Parameter	Value/Parameterisation	units	Reference
α_0	Accommodation coefficient at reference temperature	3×10^{-3} [i]	Dimensionless	Hudson et al. (2002)
k_{diff}	Diffusion coefficient of nitrate in ice	$1.37 \times 10^{-2610/T}$	$\mathrm{cm^2\,s^{-1}}$	Thibert et al. (1998)
k_w	Thermal conductivity of snow-pack	$k_w = k_{ice}\left(\frac{\rho}{\rho_{ice}}\right)^{2-0.5\frac{\rho}{\rho_{ice}}}$	$\mathrm{Wm^{-1}K^{-1}}$	Hutterli et al. (2003) therein
k_{ice}	Thermal conductivity of ice	$k_{ice} = 9.828\exp(-0.0057T)$	$\mathrm{Wm^{-1}K^{-1}}$	Hutterli et al. (2003) therein
$\Delta_{\mathrm{sol}}H$	Enthalpy of solution at standard temperature	-72.3	$\mathrm{kJ\,mol^{-1}}$	Brimblecombe and Clegg (1988)
$\Delta_{\mathrm{obs}}H$	Enthalpy of uptake	-44	$\mathrm{kJ\,mol^{-1}}$	Thomas et al. (2011)
k_{H}^0	Henry constant at 298 K	1.7×10^5 [ii]	$\mathrm{M\,atm^{-1}}$	Brimblecombe and Clegg (1988)
N_{max}	Maximum adsorption site	2.7×10^{18}	$\mathrm{molecules\,m^{-2}}$	Crowley et al. (2010)
$\overline{v}$	Mean molecular speed	$\sqrt{\frac{8\,RT}{M_m\,\pi}}$ [iii]	$\mathrm{m\,s^{-1}}$	Sander (1999)
$X_{\mathrm{HNO_3}}^0$	Molar fraction of HNO_3 in ice	$X_{\mathrm{HNO_3}}^0 = 2.37 \times 10^{-12}\exp(\frac{3532.2}{T})P_{\mathrm{HNO_3}}^{1/2.3}$	$\mathrm{mol\,mol^{-1}}$	Thibert et al. (1998)
K_{eq}	Langmuir adsorption equilibrium constant	$-8.2 \times 10^{-18}\mathrm{T} + 2.01 \times 10^{-15}$	$\mathrm{m^3 molecule^{-1}}$	Burkholder and Wine (2015)
D_v	Water vapour diffusivity	$D_v = 2.11 \times 10^{-5}(\frac{T}{T_o})^{1.94}\frac{P_o}{P}$	$\mathrm{m^2\,s^{-1}}$	Pruppacher and Klett (1997)

[i] Temperature dependent accommodation coefficient, $\alpha = \frac{\exp\{\ln(\frac{\alpha_0}{1-\alpha_0})[-\frac{\Delta_{\mathrm{obs}}H}{R}(\frac{1}{T}-\frac{1}{T_f})]\}}{1-\exp\{\ln(\frac{\alpha_0}{1-\alpha_0})[-\frac{\Delta_{\mathrm{obs}}H}{R}(\frac{1}{T}-\frac{1}{T_f})]\}}$, (Thomas et al., 2011), where R is the molar gas constant, T is the temperature, $\mathrm{T_f}$ is the reference temperature (220 K) and α_0 is the from Hudson et al. (2002) at 220 K

[ii] Temperature dependent dimensionless Henry's Law coefficient, $k_{\mathrm{H}}^{\mathrm{cc}} = k_{\mathrm{H}}^0 \times RT \times \exp\left(\frac{-\Delta_{\mathrm{sol}}H}{R}\left(\frac{1}{T}-\frac{1}{T^{\ominus}}\right)\right)$, where $T^{\ominus}$ is the standard temperature (298 K).

[iii] M_m is the molar mass of the gas.

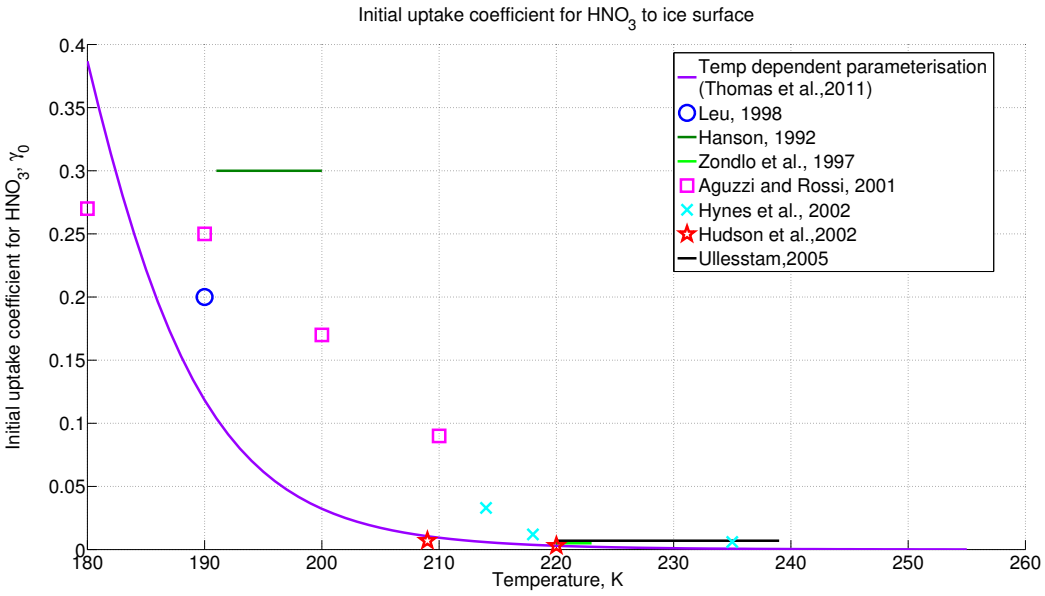

Figure A1. Initial uptake coefficient for HNO_3 as a function of temperature obtained from different studies. ~~The parameterisation used within~~ In this study the parameterisation of $\alpha(T)$ with α_0 after Hudson et al. (2002) is ~~formulated in~~ used (Table A1, solid purple line) and is chosen to give the best representation of the dependency on temperature.

~~(A) Year-round estimates of the specific surface area (SSA) of snow at Dome C (—) and Halley (– –) were interpolated from observations at Dome C during 2012-2015 by Picard et al. (2016) (×).~~
925 ~~The SSA estimates for Halley take into account the shorter cold period compare to Dome C, which tends to have larger SSA. (B) Year-round estimates of effective grain radius ($R_{\rm eff}$) at Dome C (—) and Halley (– –) derived from Eq. 6.~~

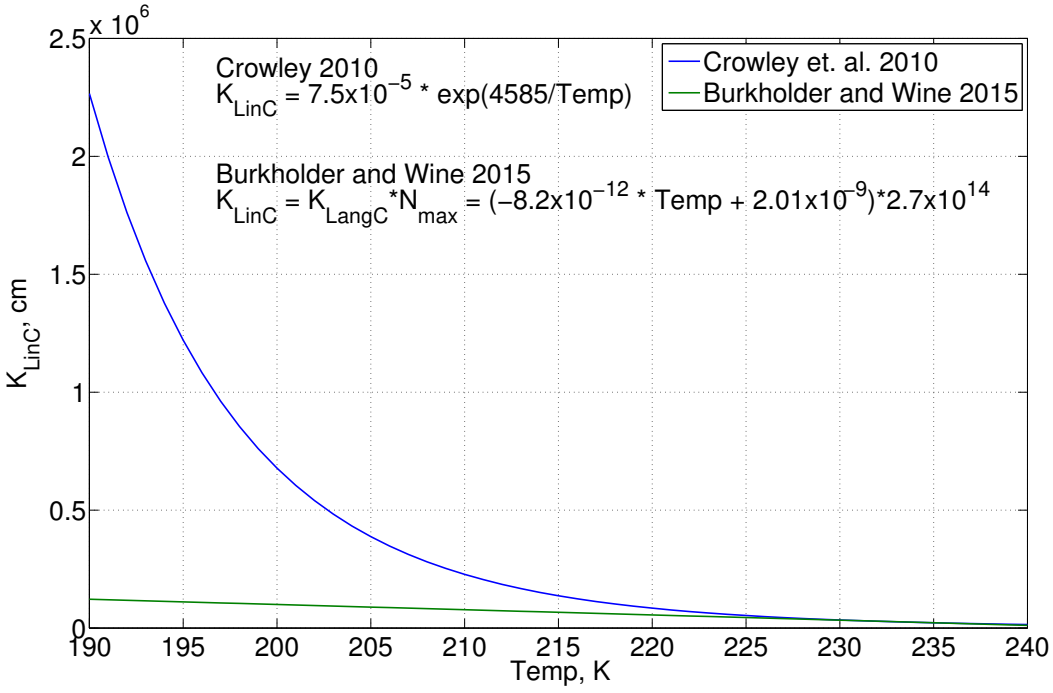

Figure A2. Langmuir adsorption equilibrium constant, $K_{\mathrm{LinC}} = K_{eq} \times N_{\max}$. The preferred temperature range for both parameterisation is 214-240 K and within this range the two parameterisations provide a comparable value. The Crowley et al. (2010) parameterisation deviate from the Burkholder and Wine (2015) parameterisation as temperature drop below 214 K due to the exponential temperature term. Here, the parameterisation from Burkholder and Wine (2015) was chosen based on the extreme cold temperature found in our validation sites (minimum winter temperature at Dome C is $\sim$ 199 K, Erbland et al., 2013).

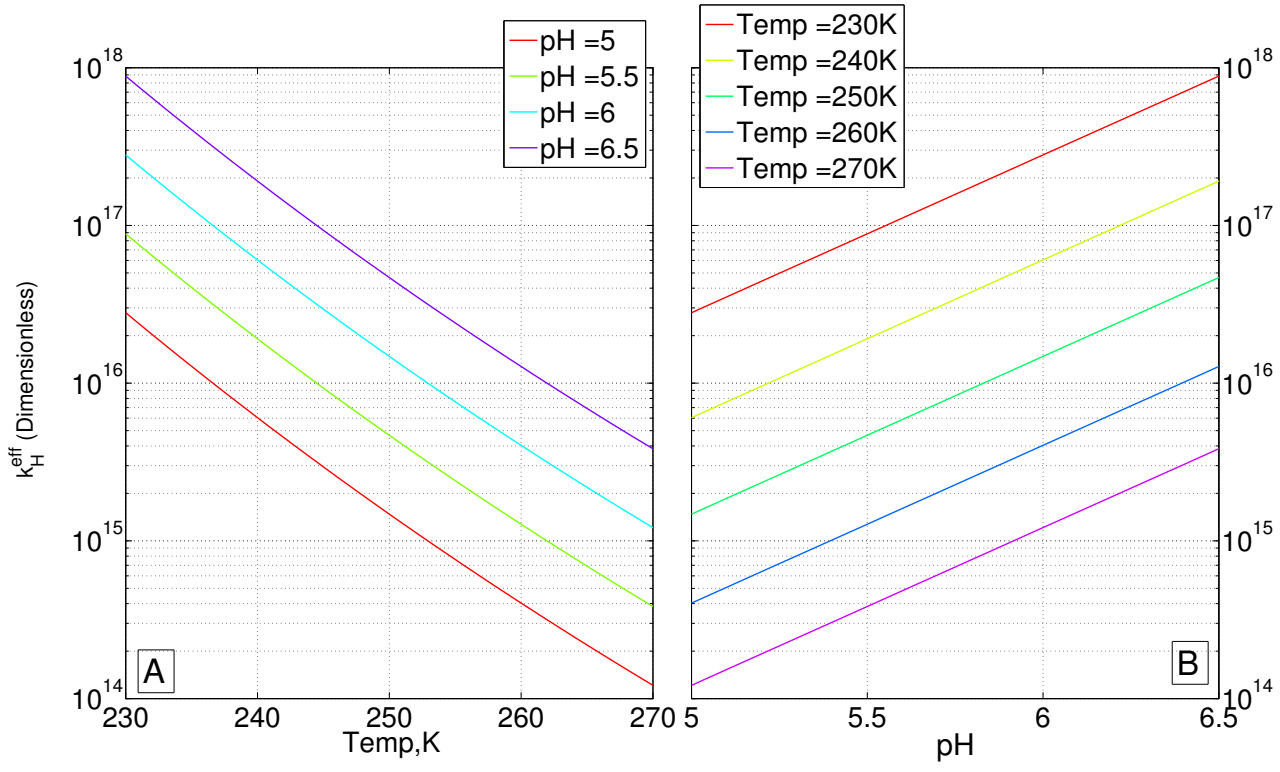

Figure A3. The dependence of the effective Henry's Law coefficient, $k_{\mathrm{H^{eff}}}$, of $\mathrm{HNO_3}$ on (A) temperature and (B) pH

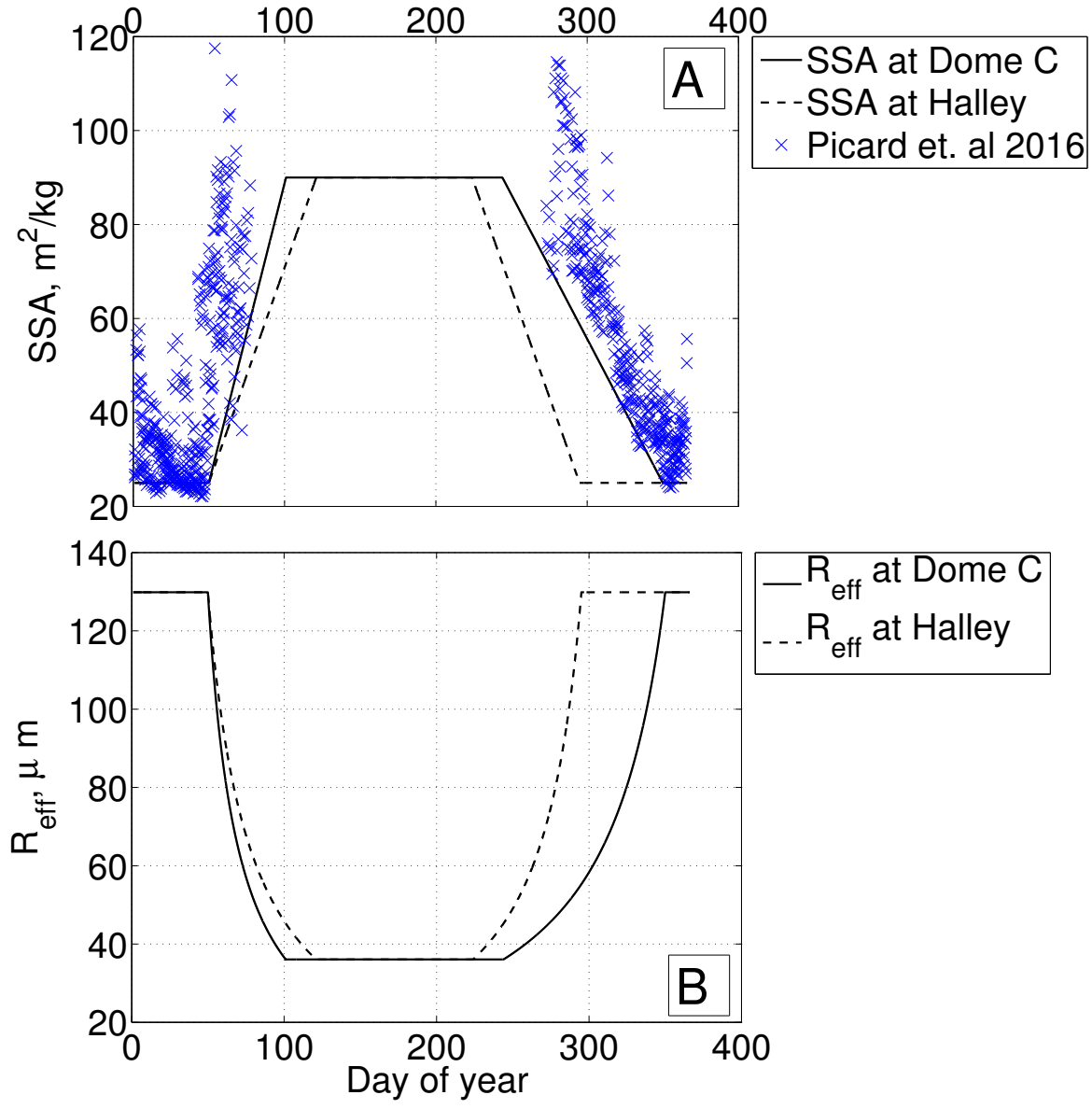

Figure A4. (**A**) Year-round estimates of the specific surface area (SSA) of snow at Dome C (−) and Halley (−−) were interpolated from observations at Dome C during 2012-2015 by Picard et al. (2016) (×). The SSA estimates for Halley take into account the shorter cold period compare to Dome C, which tends to have larger SSA. (**B**) Year-round estimates of effective grain radius (R_{eff}) at Dome C (−) and Halley (−−) derived from Eq. 6.

References

Abbatt, Jonathan P. D.: Interaction of HNO3 with ~~water?ice~~ water-ice surfaces at temperatures of the free troposphere, Geophysical Research Letters, 24, 1479–1482, doi:10.1029/97GL01403, http://dx.doi.org/10.1029/97GL01403, 1997.

Akinfiev, N. N., Mironenko, M. V., and Grant, S. A.: Thermodynamic Properties of NaCl Solutions at Subzero Temperatures, Journal of Solution Chemistry, 30, 1065–1080, doi:10.1023/A:1014445917207, http://dx.doi.org/10.1023/A:1014445917207, 2001.

Ammann, M., Cox, R. A., Crowley, J. N., Jenkin, M. E., Mellouki, A., Rossi, M. J., Troe, J., and Wallington, T. J.: Evaluated kinetic and photochemical data for atmospheric chemistry: Volume VI ? heterogeneous reactions with liquid substrates, Atmospheric Chemistry and Physics, 13, 8045–8228, doi:10.5194/acp-13-8045-2013, http://www.atmos-chem-phys.net/13/8045/2013/, 2013.

Argentini, S., Pietroni, I., Mastrantonio, G., Viola, A. P., Dargaud, G., and Petenko, I.: Observations of near surface wind speed, temperature and radiative budget at Dome C, Antarctic Plateau during 2005, Antarctic Science, 26, 104–112, doi:10.1017/S0954102013000382, 2014.

Arthern, R. J., Winebrenner, D. P., and Vaughan, D. G.: Antarctic snow accumulation mapped using polarization of 4.3-cm wavelength microwave emission, Journal of Geophysical Research: Atmospheres, 111, n/a–n/a, doi:10.1029/2004JD005667, http://dx.doi.org/10.1029/2004JD005667, d06107, 2006.

Bartels-Rausch, T., Jacobi, H.-W., Kahan, T. F., Thomas, J. L., Thomson, E. S., Abbatt, J. P. D., Ammann, M., Blackford, J. R., Bluhm, H., Boxe, C., Domine, F., Frey, M. M., Gladich, I., Guzmán, M. I., Heger, D., Huthwelker, T., Klán, P., Kuhs, W. F., Kuo, M. H., Maus, S., Moussa, S. G., McNeill, V. F., Newberg, J. T., Pettersson, J. B. C., Roeselová, M., and Sodeau, J. R.: A review of air ice chemical and physical interactions (AICI): liquids, quasi-liquids, and solids in snow, Atmospheric Chemistry and Physics, 14, 1587–1633, doi:10.5194/acp-14-1587-2014, http://www.atmos-chem-phys.net/14/1587/2014/, 2014.

Beine, H. J., Honrath, R. E., DominÈ, F., Simpson, W. R., and Fuentes, J. D.: NOx during background and ozone depletion periods at Alert: Fluxes above the snow surface, Journal of Geophysical Research: Atmospheres, 107, ACH 7–1–ACH 7–12, doi:10.1029/2002JD002082, http://dx.doi.org/10.1029/2002JD002082, 4584, 2002.

Beine, H. J., DominÈ, F., Ianniello, A., Nardino, M., Allegrini, I., Teinilä, K., and Hillamo, R.: Fluxes of nitrates between snow surfaces and the atmosphere in the European high Arctic, Atmospheric Chemistry and Physics, 3, 335–346, doi:10.5194/acp-3-335-2003, http://www.atmos-chem-phys.net/3/335/2003/, 2003.

Beyer, K. D., , and Hansen, A. R.: Phase Diagram of the Nitric Acid/Water System: Implications for Polar Stratospheric Clouds, The Journal of Physical Chemistry A, 106, 10 275–10 284, doi:10.1021/jp025535o, http://dx.doi.org/10.1021/jp025535o, 2002.

Bock, J., Savarino, J., and Picard, G.: Air–snow exchange of nitrate: a modelling approach to investigate physicochemical processes in surface snow at Dome C, Antarctica, Atmospheric Chemistry and Physics, 16, 12 531–12 550, doi:10.5194/acp-16-12531-2016, http://www.atmos-chem-phys.net/16/12531/2016/, 2016.

Boxe, C. S. and Saiz-Lopez, A.: Multiphase modeling of nitrate photochemistry in the quasi-liquid layer (QLL): implications for NO_x release from the Arctic and coastal Antarctic snowpack, Atmospheric Chemistry and Physics, 8, 4855–4864, doi:10.5194/acp-8-4855-2008, http://www.atmos-chem-phys.net/8/4855/2008/, 2008.

Brimblecombe, P. and Clegg, S. L.: The solubility and behaviour of acid gases in the marine aerosol, Journal of Atmospheric Chemistry, 7, 1–18, doi:10.1007/BF00048251, http://dx.doi.org/10.1007/BF00048251, 1988.

Burkholder,J. B. , Sander, S. P. , Abbatt, J. P., Barker, J. R., Huie, R. E., Kolb, C. E., Kurylo, M. J., Orkin, V. L., Wilmouth, D. M., Wine, P. H. : Chemical Kinetics and Photochemical Data for Use in Atmospheric Studies, Evaluation No. 18, JPL Publication 15-10, Jet Propulsion Laboratory, Pasadena, 2015.

Cho, H., Shepson, P. B., Barrie, L. A., Cowin, J. P., Zaveri, R.: NMR Investigation of the QuasiBrine Layer in Ice/Brine Mixtures, The Journal of Physical Chemistry B, 106, 11 226–11 232, doi:10.1021/jp020449, http://dx.doi.org/10.1021/jp020449+, 2002.

Conde, M. M., Vega, C., and Patrykiejew, A.: The thickness of a liquid layer on the free surface of ice as obtained from computer simulation, The Journal of Chemical Physics, 129, 014702, doi:http://dx.doi.org/10.1063/1.2940195, http://scitation.aip.org/content/aip/journal/jcp/129/1/10.1063/1.2940195, 2008.

Cox, R. A., Fernandez, M. A., Symington, A., Ullerstam, M., and Abbatt, J. P. D.: A kinetic model for uptake of HNO3 and HCl on ice in a coated wall flow system, Phys. Chem. Chem. Phys., 7, 3434–3442, doi:10.1039/B506683B, http://dx.doi.org/10.1039/B506683B, 2005.

Crowley, J. N., Ammann, M., Cox, R. A., Hynes, R. G., Jenkin, M. E., Mellouki, A., Rossi, M. J., Troe, J., and Wallington, T. J.: Evaluated kinetic and photochemical data for atmospheric chemistry: Volume V heterogeneous reactions on solid substrates, Atmospheric Chemistry and Physics, 10, 9059–9223, doi:10.5194/acp-10-9059-2010, http://www.atmos-chem-phys.net/10/9059/2010/, 2010.

Dasgupta, P. K., Campbell, S. W., Al-Horr, R. S., Ullah, S. R., Li, J., Amalfitano, C., and Poor, N. D.: Conversion of sea salt aerosol to NaNO3 and the production of HCl: Analysis of temporal behavior of aerosol chloride/nitrate and gaseous HCl/HNO3 concentrations with {AIM}, Atmospheric Environment, 41, 4242 – 4257, doi:http://dx.doi.org/10.1016/j.atmosenv.2006.09.054, http://www.sciencedirect.com/science/article/pii/S1352231006012921, (BRACE)Bay Region Atmospheric Chemistry Experiment, 2007.

Domine, F., Bock, J., Voisin, D., and Donaldson, D. J.: Can We Model Snow Photochemistry? Problems with the Current Approaches, The Journal of Physical Chemistry A, 117, 4733–4749, doi:10.1021/jp3123314, http://dx.doi.org/10.1021/jp3123314, pMID: 23597185, 2013.

Erbland, J., Vicars, W. C., Savarino, J.,Morin, S., Frey, M. M., Frosini, D., Vince, E., Martins, J. M. F.: Air snow transfer of nitrate on the East Antarctic Plateau Part 1: Isotopic evidence for a photolytically driven dynamic equilibrium in summer , Atmospheric Chemistry and Physics, 13, 6403–6419, doi:10.5194/acp-13-6403-2013, http://www.atmos-chem-phys.net/13/6403/2013/, 2013.

Finlayson-Pitts, B. J. and Jr., J. N. P.: {CHAPTER} 5 - Kinetics and Atmospheric Chemistry, in: Chemistry of the Upper and Lower Atmosphere, edited by Finlayson-Pitts, B. J. and Pitts, J. N., pp. 130 – 178, Academic Press, San Diego, doi:http://dx.doi.org/10.1016/B978-012257060-5/50007-1, http://www.sciencedirect.com/science/article/pii/B9780122570605500071, 2000.

Fowler, D., Amann, M., Anderson, F., Ashmore, M., Cox, P., Depledge, M., Derwent, D., Grennfelt, P., Hewitt, N., Hov, O., Jenkin, M., Kelly, F., Liss, P. S., Pilling, M., Pyle, J., Slingo, J. and Stevenson, D.: Ground-level ozone in the 21st century: future trends, impacts and policy implications, vol. 15/08 of *Science Policy*, The Royal Society, London, http://nora.nerc.ac.uk/8577/, prof. David Fowler was Chair of the Working Group, 2008.

France, J. L., King, M. D., Frey, M. M., Erbland, J., Picard, G., Preunkert, S., MacArthur, A., and Savarino, J.: Snow optical properties at Dome C (Concordia), Antarctica; implications for snow emissions and snow chemistry of reactive nitrogen, Atmospheric Chemistry and Physics, 11, 9787–9801, doi:10.5194/acp-11-9787-2011, http://www.atmos-chem-phys.net/11/9787/2011/, 2011.

Frey, M. M., Savarino, J., Morin, S., Erbland, J., and Martins, J. M. F.: Photolysis imprint in the nitrate stable isotope signal in snow and atmosphere of East Antarctica and implications for reactive nitrogen cycling, Atmospheric Chemistry and Physics, 9, 8681–8696, doi:10.5194/acp-9-8681-2009, http://www.atmos-chem-phys.net/9/8681/2009/, 2009.

Frey, M. M., Brough, N., France, J. L., Anderson, P. S., Traulle, O., King, M. D., Jones, A. E., Wolff, E. W., and Savarino, J.: The diurnal variability of atmospheric nitrogen oxides (NO and NO_2) above the Antarctic Plateau driven by atmospheric stability and snow emissions, Atmospheric Chemistry and Physics, 13, 3045–3062, doi:10.5194/acp-13-3045-2013, http://www.atmos-chem-phys.net/13/3045/2013/, 2013.

Flanner, M. G. and Zender, C. S.: Linking snowpack microphysics and albedo evolution, Journal of Geophysical Research: Atmospheres, 111, n/a–n/a, doi:10.1029/2005JD006834, http://dx.doi.org/10.1029/2005JD006834, d12208, 2006.

Gligorovski, S., Strekowski, R., Barbati, S., and Vione, D.: Environmental Implications of Hydroxyl Radicals (OH), Chemical Reviews, 115, 13 051–13 092, doi:10.1021/cr500310b, http://dx.doi.org/10.1021/cr500310b, pMID: 26630000, 2015.

Grannas, A. M., Jones, A. E., Dibb, J., Ammann, M., Anastasio, C., Beine, H. J., Bergin, M., Bottenheim, J., Boxe, C. S., Carver, G., Chen, G., Crawford, J. H., Dominé, F., Frey, M. M., Guzmán, M. I., Heard, D. E., Helmig, D., Hoffmann, M. R., Honrath, R. E., Huey, L. G., Hutterli, M., Jacobi, H. W., Klán, P., Lefer, B., McConnell, J., Plane, J., Sander, R., Savarino, J., Shepson, P. B., Simpson, W. R., Sodeau, J. R., von Glasow, R., Weller, R., Wolff, E. W., and Zhu, T.: An overview of snow photochemistry: evidence, mechanisms and impacts, Atmospheric Chemistry and Physics, 7, 4329–4373, doi:10.5194/acp-7-4329-2007, http://www.atmos-chem-phys.net/7/4329/2007/, 2007.

Honrath, R. E., Peterson, M. C., Dziobak, M. P., Dibb, J. E., Arsenault, M. A., and Green, S. A.: Release of NOx from sunlight-irradiated midlatitude snow, Geophysical Research Letters, 27, 2237–2240, doi:10.1029/1999GL011286, http://dx.doi.org/10.1029/1999GL011286, 2000.

Hudson, P. K., Zondlo, M. A., , and Tolbert*, M. A.: The Interaction of Methanol, Acetone, and Acetaldehyde with Ice and Nitric Acid-Doped Ice: Implications for Cirrus Clouds, The Journal of Physical Chemistry A, 106, 2882–2888, doi:10.1021/jp012718m, http://dx.doi.org/10.1021/jp012718m, 2002.

Huthwelker, T. , Malmström, M. E., Helleis, F. , Moortgat, G. K. and Peter, T.: , Kinetics of HCl Uptake on Ice at 190 and 203 K: Implications for the Microphysics of the Uptake Process, The Journal of Physical Chemistry A, 30, 6302–6318, doi:10.1021/jp0309623, http://dx.doi.org/10.1021/jp0309623, 2004.

Huthwelker, T. and Ammann, M. and Peter, T.: , The Uptake of Acidic Gases on Ice, Chemical Reviews, 106, 1375-1444, doi:10.1021/cr020506v, http://dx.doi.org/10.1021/cr020506v, 2006.

Hutterli, M. A. and Röthlisberger, R.: Atmosphere-to-snow-to-firn transfer studies of HCHO at Summit, Greenland, GEOPHYSICAL RESEARCH LETTERS, 26, 1691–1694, 1999.

Hutterli, M. A., McConnell, J. R., Bales, R. C., and Stewart, R. W.: Sensitivity of hydrogen peroxide (H2O2) and formaldehyde (HCHO) preservation in snow to changing environmental conditions: Impli-

cations for ice core records, Journal of Geophysical Research: Atmospheres, 108, ACH 6–1–ACH 6–9, doi:10.1029/2002JD002528, http://dx.doi.org/10.1029/2002JD002528, 4023, 2003.

Jacobson, M. Z.: Fundamentals of Atmospheric Modeling, Cambridge University Press, https://books.google.co.uk/books?id=96wWzoyKRMoC, 2005.

Jones, A. E., Weller, R., Anderson, P. S., Jacobi, H.-W., Wolff, E. W., Schrems, O., and Miller, H.: Measurements of NOx emissions from the Antarctic snowpack, Geophysical Research Letters, 28, 1499–1502, doi:10.1029/2000GL011956, http://dx.doi.org/10.1029/2000GL011956, 2001.

Jones, A. E., Wolff, E. W., Salmon, R. A., Bauguitte, S. J.-B., Roscoe, H. K., Anderson, P. S., Ames, D., Clemitshaw, K. C., Fleming, Z. L., Bloss, W. J., Heard, D. E., Lee, J. D., Read, K. A., Hamer, P., Shallcross, D. E., Jackson, A. V., Walker, S. L., Lewis, A. C., Mills, G. P., Plane, J. M. C., Saiz-Lopez, A., Sturges, W. T., and Worton, D. R.: Chemistry of the Antarctic Boundary Layer and the Interface with Snow: an overview of the CHABLIS campaign, Atmospheric Chemistry and Physics, 8, 3789–3803, doi:10.5194/acp-8-3789-2008, http://www.atmos-chem-phys.net/8/3789/2008/, 2008.

Jones, A. E., Wolff, E. W., Ames, D., Bauguitte, S. J.-B., Clemitshaw, K. C., Fleming, Z., Mills, G. P., Saiz-Lopez, A., Salmon, R. A., Sturges, W. T., and Worton, D. R.: The multi-seasonal NO_y budget in coastal Antarctica and its link with surface snow and ice core nitrate: results from the CHABLIS campaign, Atmospheric Chemistry and Physics, 11, 9271–9285, doi:10.5194/acp-11-9271-2011, http://www.atmos-chem-phys.net/11/9271/2011/, 2011.

Jourdain, B., Preunkert, S., Cerri, O., Castebrunet, H, Udisti, R. and Legrand, M.: Year-round record of size-segregated aerosol composition in central Antarctica (Concordia station): Implications for the degree of fractionation of sea-salt particles, Journal of Geophysical Research: Atmospheres, 113, D14308, doi:10.1029/2007JD009584 , http://dx.doi.org/10.1029/2007JD009584, 2008.

Kuo, M. H., Moussa, S. G., and McNeill, V. F.: Modeling interfacial liquid layers on environmental ices, Atmospheric Chemistry and Physics, 11, 9971–9982, doi:10.5194/acp-11-9971-2011, http://www.atmos-chem-phys.net/11/9971/2011/, 2011.

Legrand, M., Yang, X., Preunkert, S., and Theys, N.: Year-round records of sea salt, gaseous, and particulate inorganic bromine in the atmospheric boundary layer at coastal (Dumont d'Urville) and central (Concordia) East Antarctic sites, Journal of Geophysical Research: Atmospheres, 121, 997–1023, doi:10.1002/2015JD024066, http://dx.doi.org/10.1002/2015JD024066, 2015JD024066, 2016.

McConnell, J. R., Bales, R. C., Stewart, R. W., Thompson, A. M., Albert, M. R., and Ramos, R.: Physically based modeling of atmosphere-to-snow-to-firn transfer of H2O2 at South Pole, Journal of Geophysical Research: Atmospheres, 103, 10 561–10 570, doi:10.1029/98JD00460, http://dx.doi.org/10.1029/98JD00460, 1998.

McNeill, V. F., Grannas, A. M., Abbatt, J. P. D., Ammann, M., Ariya, P., Bartels-Rausch, T., Domine, F., Donaldson, D. J., Guzman, M. I., Heger, D., Kahan, T. F., Klán, P., Masclin, S., Toubin, C., and Voisin, D.: Organics in environmental ices: sources, chemistry, and impacts, Atmospheric Chemistry and Physics, 12, 9653–9678, doi:10.5194/acp-12-9653-2012, http://www.atmos-chem-phys.net/12/9653/2012/, 2012.

Morin, S., Savarino, J., Frey, M. M., Yan, N., Bekki, S., Bottenheim, J. W., and Martins, J. M. F.: Tracing the Origin and Fate of NOx in the Arctic Atmosphere Using Stable Isotopes in Nitrate, Science, 322, 730–732, doi:10.1126/science.1161910, http://science.sciencemag.org/content/322/5902/730, 2008.

Murray, K. A., Kramer, L. J., Doskey, P. V., Ganzeveld, L., Seok, B., Dam, B. V., and Helmig, D.: Dynamics of ozone and nitrogen oxides at Summit, Greenland. II. Simulating snowpack chemistry during a spring high ozone event with a 1-D process-scale model, Atmospheric Environment, 117, 110 – 123, doi:http://dx.doi.org/10.1016/j.atmosenv.2015.07.004, http://www.sciencedirect.com/science/article/pii/S135223101530203X, 2015.

Picard, G., Libois, Q., Arnaud, L., Vérin, G., and Dumont, M.: Time-series of snow spectral albedo and superficial snow specific surface area at Dome C in Antarctica, 2012-2015, doi:10.1594/PANGAEA.860945, https://doi.pangaea.de/10.1594/PANGAEA.860945, supplement to: Picard, G et al. (2016): Development and calibration of an automatic spectral albedometer to estimate near-surface snow SSA time series. The Cryosphere, 10(3), 1297-1316, doi:10.5194/tc-10-1297-2016, 2016.

Pinzer, B. R., Schneebeli, M., and Kaempfer, T. U.: Vapor flux and recrystallization during dry snow metamorphism under a steady temperature gradient as observed by time-lapse micro-tomography, The Cryosphere, 6, 1141–1155, doi:10.5194/tc-6-1141-2012, http://www.the-cryosphere.net/6/1141/2012/, 2012.

Press, .W. H, Teukolsky, S. A., Vetterling, W. T., F.lannery, B. P.: Numerical Recipe in Fortran 90, Cambridge Univeristy Press, 2 edn., 1996.

Pruppacher, H. R. and Klett, James D., .: Microphysics of clouds and precipitation, Dordrecht ; Boston : Kluwer Academic Publishers, 2nd rev. and enl. ed edn., "With an introduction to cloud chemistry and cloud electricity.", 1997.

Rankin, A. M. and Wolff, E. W.: A year-long record of size-segregated aerosol composition at Halley, Antarctica, Journal of Geophysical Research: Atmospheres, 108, D24, 4775 doi:10.1029/2003JD003993, http://dx.doi.org/10.1029/2003JD003993, 2003.

Röthlisberger, R., Hutterli, M. A., Sommer, S., Wolff, E. W., and Mulvaney, R.: Factors controlling nitrate in ice cores: Evidence from the Dome C deep ice core, Journal of Geophysical Research: Atmospheres, 105, 20 565–20 572, doi:10.1029/2000JD900264, http://dx.doi.org/10.1029/2000JD900264, 2000.

Sander, R.: Modeling Atmospheric Chemistry: Interactions between Gas-Phase Species and Liquid Cloud/Aerosol Particles, Surveys in Geophysics, 20, 1–31, doi:10.1023/A:1006501706704, http://dx.doi.org/10.1023/A:1006501706704, 1999.

Sander, R.: Compilation of Henry's law constants (version 4.0) for water as solvent, Atmospheric Chemistry and Physics, 15, 4399–4981, doi:10.5194/acp-15-4399-2015, http://www.atmos-chem-phys.net/15/4399/2015/, 2015.

Sazaki, G, and Zepeda S, Nakatsubo S, Yokomine. M. Furukawa. Y.: Quasi-liquid layers on ice crystal surfaces are made up of two different phases, Proc Natl Acad Sci U S A., 4, 1052–1055, doi:10.1073/pnas.1116685109, 2012.

Tang, M. J., Cox, R. A., and Kalberer, M.: Compilation and evaluation of gas phase diffusion coefficients of reactive trace gases in the atmosphere: volume 1. Inorganic compounds, Atmospheric Chemistry and Physics, 14, 9233–9247, doi:10.5194/acp-14-9233-2014, http://www.atmos-chem-phys.net/14/9233/2014/, 2014.

Thibert, E., , and Dominé, F.: Thermodynamics and Kinetics of the Solid Solution of HNO3 in Ice, The Journal of Physical Chemistry B, 102, 4432–4439, doi:10.1021/jp980569a, http://dx.doi.org/10.1021/jp980569a, 1998.

Thomas, J. L., Stutz, J., Lefer, B., Huey, L. G., Toyota, K., Dibb, J. E., and von Glasow, R.: Modeling chemistry in and above snow at Summit, Greenland? Part 1: Model description and results, Atmospheric Chemistry and Physics, 11, 4899–4914, doi:10.5194/acp-11-4899-2011, http://www.atmos-chem-phys.net/11/4899/2011/, 2011.

Toyota, K., McConnell, J. C., Staebler, R. M., and Dastoor, A. P.: Air-snowpack exchange of bromine, ozone and mercury in the springtime Arctic simulated by the 1-D model PHANTAS - Part 1 In-snow bromine activation and its impact on ozone, Atmospheric Chemistry and Physics, 14, 4101–4133, doi:10.5194/acp-14-4101-2014, http://www.atmos-chem-phys.net/14/4101/2014/, 2014.

Traversi, R., Udisti, R., Frosini, D., Becagli, S., Ciardini, V., Funke, B., Lanconelli, C., Petkov, B., Scarchilli, C., Severi, M., and Vitale, V.: Insights on nitrate sources at Dome C (East Antarctic Plateau) from multi-year aerosol and snow records, Tellus B, 66, http://www.tellusb.net/index.php/tellusb/article/view/22550, 2014.

Waddington, E. D., Cunningham, J., and Harder, S. L.: The Effects Of Snow Ventilation on Chemical Concentrations, pp. 403–451, Springer Berlin Heidelberg, Berlin, Heidelberg, doi:10.1007/978-3-642-61171-1_18, http://dx.doi.org/10.1007/978-3-642-61171-1_18, 1996.

Wolff, E. W., Jones, A. E., Bauguitte, S. J.-B., and Salmon, R. A.: The interpretation of spikes and trends in concentration of nitrate in polar ice cores, based on evidence from snow and atmospheric measurements, Atmospheric Chemistry and Physics, 8, 5627–5634, doi:10.5194/acp-8-5627-2008, http://www.atmos-chem-phys.net/8/5627/2008/, 2008.

Udisti, R., Becagli, S., Benassai, S., Castellano, E., Fattori, I., Innocenti, M., Migliori, A., and Traversi, R.: Atmospheresnow interaction by a comparison between aerosol and uppermost snow-layers composition at Dome C, East Antarctica, Annals of Glaciology, 39, 53–61, doi:doi:10.3189/172756404781814474, http://www.ingentaconnect.com/content/igsoc/agl/2004/00000039/00000001/art00010, 2004.

Ullerstam, M. and Abbatt, J. P. D.: Burial of gas-phase HNO3 by growing ice surfaces under tropospheric conditions, Phys. Chem. Chem. Phys., 7, 3596–3600, doi:10.1039/B507797D, http://dx.doi.org/10.1039/B507797D, 2005a.

Ullerstam, M., Thornberry, T., and Abbatt, J. P. D.: Uptake of gas-phase nitric acid to ice at low partial pressures: evidence for unsaturated surface coverage, Faraday Discuss., 130, 211–226, doi:10.1039/B417418F, http://dx.doi.org/10.1039/B417418F, 2005b.

Yuan-Hui, L. and Gregory, S.: Diffusion of ions in sea water and in deep-sea sediments, Geochimica et Cosmochimica Acta, 38, 703 – 714, doi:http://dx.doi.org/10.1016/0016-7037(74)90145-8, http://www.sciencedirect.com/science/article/pii/0016703774901458, 1974.